REPORT SNO 4838

MyLake (v.1.1)

Technical model documentation and user's guide for version 1.1

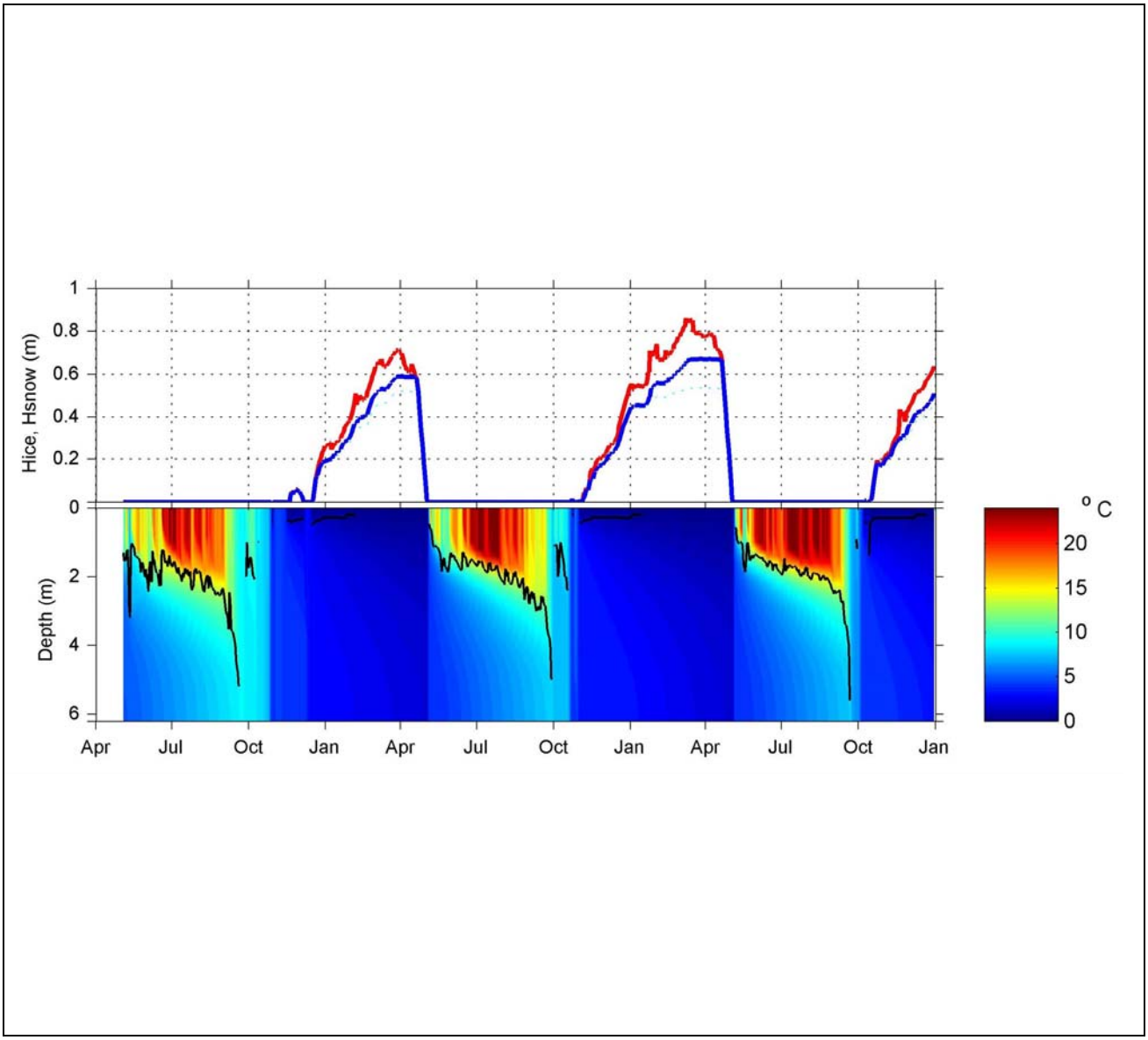

Norwegian Institute for Water Research
– an institute in the Environmental Research Alliance of Norway

REPORT

Main Office
P.O. Box 173, Kjelsås
N-0411 Oslo, Norway
Phone (47) 22 18 51 00
Telefax (47) 22 18 52 00
Internet: www.niva.no

Regional Office, Sørlandet
Televeien 3
N-4879 Grimstad, Norway
Phone (47) 37 29 50 55
Telefax (47) 37 04 45 13

Regional Office, Østlandet
Sandvikaveien 41
N-2312 Ottestad, Norway
Phone (47) 62 57 64 00
Telefax (47) 62 57 66 53

Regional Office, Vestlandet
Nordnesboder 5
N-5008 Bergen, Norway
Phone (47) 55 30 22 50
Telefax (47) 55 30 22 51

Akvaplan-NIVA A/S
N-9005 Tromsø, Norway
Phone (47) 77 68 52 80
Telefax (47) 77 68 05 09

Title	Serial No.	Date
MyLake (v.1.1): Technical model documentation and user's guide for version 1.1	4838	28. 5. 2004
	Report No. Sub-No.	Pages Price
		44
Author(s)	Topic group	Distribution
Tuomo M. Saloranta and Tom Andersen		
	Geographical area	Printed
		NIVA

Client(s)	Client ref.

Abstract

MyLake (Multi-year simulation model for Lake thermo- and phytoplankton dynamics) is a one-dimensional process-based model code for simulation of daily 1) vertical distribution of lake water temperature and thus stratification, 2) evolution of seasonal lake ice and snow cover, and 3) phosphorus-phytoplankton dynamics. MyLake has a relatively simple and transparent model structure, it is easy to set up, and is suitable both for making predictions and scenarios, and to be used as an investigative tool. Short runtime allows application of comprehensive sensitivity and uncertainty analysis as well as simulation of a large number of lakes or over long periods (decades). MyLake aims to include only the most significant physical, chemical and biological processes in a well-balanced and robust way. The technical part of this report (sections 2-4 and Appendix A) gives a detailed description of the different processes and algorithms included in MyLake (v.1.1) model code. Section 5 gives brief instructions for setting up and running a MyLake (v.1.1) model application, while in section 6 some examples of MyLake model output are presented.

4 keywords, Norwegian	4 keywords, English
1. modellering	1. modelling
2. innsjø	2. lake
3. eutrofiering	3. eutrophication
4. MyLake	4. MyLake

Project manager Research manager Head of research department

ISBN 82-577-4520-0

MyLake (v.1.1)

Technical model documentation and user's guide for version 1.1

Preface

We thank Birger Bjerkeng for his valuable comments on this report and the Norwegian Institute for Water Research (NIVA) for funding the MyLake model development work. The application and testing of MyLake model (v.1.1) was done mainly within the project ”Benchmark models for the water framework directive” (BMW; contract no: EVK1 - CT2001-00093) funded by the Commission of European Communities, the Research Council of Norway, and NIVA.

Oslo, 28. 5. 2004

Tuomo M. Saloranta

Contents

Summary

MyLake (Multi-year simulation model for Lake thermo- and phytoplankton dynamics) is a one-dimensional process-based model code for simulation of daily 1) vertical distribution of lake water temperature and thus stratification, 2) evolution of seasonal lake ice and snow cover, and 3) phosphorus-phytoplankton dynamics. MyLake has a relatively simple and transparent model structure, it is easy to set up, and is suitable both for making predictions and scenarios, and to be used as an investigative tool. Short runtime allows application of comprehensive sensitivity and uncertainty analysis as well as simulation of a large number of lakes or over long periods (decades). MyLake aims to include only the most significant physical, chemical and biological processes in a well-balanced and robust way. The technical part of this report (sections 2-4 and Appendix A) gives a detailed description of the different processes and algorithms included in MyLake (v.1.1) model code. Section 5 gives brief instructions for setting up and running a MyLake (v.1.1) model application, while in section 6 some examples of MyLake model output are presented.

1. Introduction

MyLake (Multi-year simulation model for Lake thermo- and phytoplankton dynamics) is a one-dimensional process-based model code for simulation of daily 1) vertical distribution of lake water temperature and thus stratification, 2) evolution of seasonal lake ice and snow cover, and 3) phosphorus-phytoplankton dynamics. The lake water simulation part of the model code is based on Ford and Stefan (1980), Riley and Stefan (1988), and Hondzo and Stefan (1993), while the ice simulation code is based on Leppäranta (1991) and Saloranta (2000). MyLake has been recently developed at the Norwegian Institute for Water Research (NIVA), and the model has so far (spring 2004) been applied in BMW, THERMOS and EUROLIMPACS projects (Saloranta et al. 2004, Lydersen et al. 2003). The overall structure of MyLake model code is shown in Table 1.

Strengths of MyLake model code include:

- MyLake has a relatively simple and transparent model structure, it is easy to set up, and is suitable both for making predictions and scenarios, and to be used as an investigative tool.
- Short runtime allows application of comprehensive sensitivity and uncertainty analysis as well as simulation of a large number of lakes or over long periods (decades).
- MyLake aims to include only the most significant physical, chemical and biological processes in a well-balanced and robust way.

There are, of course, limitations too. MyLake is a newcomer and only two previous applications were documented at the time this report went to print. More applications are needed before the model code can be said to be thoroughly tested in practise. However, the model building blocks are based on more or less well-established science and have been used previously in numerous applications. Some users may also consider the model too simple for their purposes, as many processes, e.g. zooplankton grazing and detailed water-sediment nutrient feedbacks, are left out of the current version (v.1.1) of the model code. Other limitations may be the model time step which is preset to 24 hours and cannot be changed, as well as the 1-dimensional vertical resolution approach, which may not be so well suited for some particular types of problems and lakes.

Generally MyLake model code development aims to take into account the following five criteria adapted from Riley and Stefan (1988): 1) that the model code be general for use on different sites with minimum of alterations, 2) that the model code be capable of simulating a wide range of treatment options, 3) that the model code incorporate the dominant physical, chemical and biological processes, especially processes directly affected by various treatment options, 4) that the physical, chemical and biological components be modelled with similar orders of detail to reduce the possibility of a weak

link in the modelling process, and 5) that the model be economical enough to run to serve as management tool.

The technical part of this report (sections 2-4 and Appendix A) gives a detailed description of the different processes and algorithms included in the MyLake (v.1.1) model code. Section 5 gives brief instructions for setting up and running a MyLake (v.1.1) model application, and in section 6 some examples of MyLake model output are presented.

2. Modelling of lake water thermodynamics

2.1 Solving the temperature profile in water

The heat conservation equation for the temperature distribution in a horizontally homogeneous, vertically stratified lake can be written as

$$A\frac{\partial T}{\partial t} = \frac{\partial}{\partial z}\left[KA\frac{\partial T}{\partial z}\right] + A\frac{Q^*}{\rho_w C_p} \qquad (1)$$

where the first right-hand side term is the effect of diffusive mixing processes, while the second term is the effect of local heating. Temperature T [°C], vertical diffusion coefficient K [$m^2\ d^{-1}$], and local heating rate Q^* [$J\ m^{-3}\ d^{-1}$] are all functions of depth z and time t, while area A [m^2] is a function of depth alone. Heat and temperature are related through the specific heat capacity of water C_p [$J\ kg^{-1}\ °C^{-1}$] and the density of water ρ_w [$kg\ m^{-3}$], which is function of temperature.

If we partition the vertical dimension into *n* horizontal slices at depths $z_1 \ldots z_{n+1}$, starting at the surface with $z_1 = 0$, then the volume of layer *i* ($z_i \le z < z_{i+1}$) (Figure 1) will be given by

$$V_i = \int_{z_i}^{z_{i+1}} A dz \qquad (2)$$

Likewise, the heat content of a given slice can be written as

$$H_i = \rho_w C_p \int_{z_i}^{z_{i+1}} AT dz = \rho_w C_p \overline{T}_i \int_{z_i}^{z_{i+1}} A dz = \rho_w C_p V_i \overline{T}_i \qquad (3)$$

where $\overline{T}_i$ is the volume-averaged temperature of layer *i*, and the second identity is based on the definition of mean value, i.e., $\overline{T}_i = V_i^{-1} \int ATdz$. If we assume that layers maintain constant volume ($dV_i/dt = 0$), then we can also write the rate of change of the heat content of layer *i* as

$$\frac{dH_i}{dt} = \rho_w C_p \int_{z_i}^{z_{i+1}} A \frac{\partial T}{\partial t} dz = \rho_w C_p V_i \frac{d\overline{T}_i}{dt} \tag{4}$$

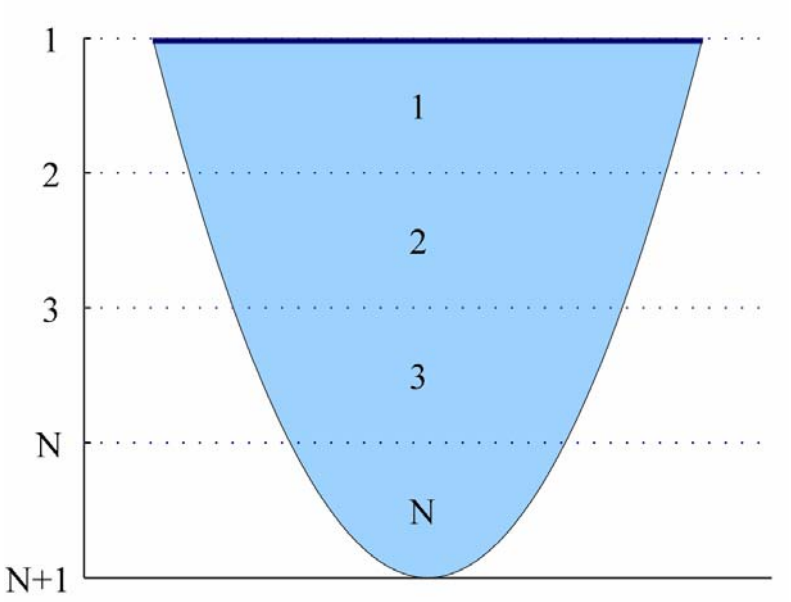

Figure 1. *Numbering of levels and water layers in MyLake model code. Some variables such as horizontal area, depth, and diffusion coefficient, are evaluated at the layer interfaces (numbering on the y-axis), while volume and most of the model's state variables, such as temperature and concentration of chlorophyll a, represent mean values for the water layers and thus can be thought to be evaluated in the middle of a layer (numbering inside the grey area denoting the lake).*

Integrating (1) from z_i to z_{i+1} gives

$$\begin{aligned} V_i \frac{d\overline{T}_i}{dt} &= \int_{z_i}^{z_{i+1}} A \frac{\partial T}{\partial t} dz \\ &= \int_{z_i}^{z_{i+1}} \frac{\partial}{\partial z}\left[KA \frac{\partial T}{\partial z} \right] dz + \int_{z_i}^{z_{i+1}} A \frac{Q^*}{\rho_w C_p} dz \\ &= \left[KA \frac{\partial T}{\partial z} \right]_{z=z_{i+1}} - \left[KA \frac{\partial T}{\partial z} \right]_{z=z_i} + V_i \frac{\overline{Q}^*_i}{\rho_w C_p} \end{aligned} \tag{5}$$

Table 1. Overview of MyLake model code structure

(Start)

For one model time step (24 h):

- Calculate surface heat fluxes and wind stress, light attenuation, and phytoplankton growth and loss rates
- Calculate profile of the diffusion coefficient *K*
- Calculate the heat flux between water and sediment (taken as heat source/sink for each layer)
- Solve new profile for each state variable taking into account advection, diffusion and local sources/sinks. Solving is done in following order: 1) temperature, 2) tracers, 3) chlorophyll *a*, 4) particulate phosphorus, 5) dissolved phosphorus.
- Update content of the sediment stores of chlorophyll *a* and particulate phosphorus

If no ice

- Check for (and possibly proceed) autumn/spring turnover

If ice cover

If $T_a<T_f$ *(freezing)*

- Calculate ice surface temperature (depending on snow cover, or ice thickness if snow is absent)
- Calculate snow ice formation in case of isostatic imbalance
- Calculate congelation ice growth by Stefan's law
- Accumulate new snow fall and subtract formed snow ice from snow cover

If $T_a \geq T_f$ *(melting)*

- Melt snow or ice from top with total surface heat flux

- Melt ice from bottom with the heat diffused to the surface layer (keeping the surface layer temperature at freezing point)
- Update snow density

- Add river inflow and update profiles of the state variables accordingly
- Mix unstable layers until stable density profile
- Mix water layers with the available turbulent kinetic energy *TKE* (*TKE*=0 under ice cover)
- Check for supercooled layers and turn them into (initial) ice
- Save results to output matrices

(Goto Start)

where $\overline{Q}^*{}_i = V_i^{-1}\int AQ^* dz$ is the layer-averaged heating rate, defined equivalently with $\overline{T}_i$. In order to represent the set of layer heat balance equations with a system of linear equations, we need to approximate the temporal and spatial derivatives with finite differences over the time and depth increments, Δt (=24 h) and Δz

$$\frac{d\overline{T}_i}{dt} \approx \frac{1}{\Delta t}\left[\overline{T}_i(t) - \overline{T}_i(t-\Delta t)\right] \tag{6a}$$

$$\left[KA\frac{\partial T}{\partial z}\right]_{z=z_i} \approx K_i A_i \frac{1}{\Delta z}\left[\overline{T}_i(t) - \overline{T}_{i-1}(t)\right] \tag{6b}$$

$$\left[KA\frac{\partial T}{\partial z}\right]_{z=z_{i+1}} \approx K_{i+1} A_{i+1} \frac{1}{\Delta z}\left[\overline{T}_{i+1}(t) - \overline{T}_i(t)\right] \tag{6c}$$

where $K_i = K(z_i)$ is interpreted as the vertical diffusion coefficient at the interface between layers i and $i-1$ (Figure 1). For the spatial derivative, these equations approximate the mid-depth temperature in each layer by the volume averaged temperature. Substitution into (4) gives

$$\begin{aligned}&\frac{V_i}{\Delta t}\left[\overline{T}_i(t) - \overline{T}_i(t-\Delta t)\right] \\ &= K_{i+1}A_{i+1}\frac{1}{\Delta z}\left[\overline{T}_{i+1}(t) - \overline{T}_i(t)\right] - K_i A_i \frac{1}{\Delta z}\left[\overline{T}_i(t) - \overline{T}_{i-1}(t)\right] + V_i \frac{\overline{Q}^*{}_i}{\rho_w C_p}\end{aligned} \tag{7}$$

Dividing through with $V_i/\Delta t$ and introducing the notation

$$\begin{aligned}\alpha_i &= \frac{\Delta t}{\Delta z}\frac{A_i}{V_i}K_i \\ \beta_i &= \frac{\Delta t}{\Delta z}\frac{A_{i+1}}{V_i}K_{i+1}\end{aligned} \tag{8}$$

(5) can be written as

$$\overline{T}_i(t) - \overline{T}_i(t-\Delta t) = \beta_i\left[\overline{T}_{i+1}(t) - \overline{T}_i(t)\right] - \alpha_i\left[\overline{T}_i(t) - \overline{T}_{i-1}(t)\right] + \Delta T_i(t) \tag{9}$$

where $\Delta T_i(t) = \left(\overline{Q}^*{}_i(t)\,\rho^{-1}C_p^{-1}\right)\Delta t$ is the temperature change due to heating in layer *i* over the time interval Δt. Rearranging so that all terms involving $\overline{T}(t)$ appear on the left-hand side gives

$$-\alpha_i\overline{T}_{i-1}(t)+(1+\alpha_i+\beta_i)\overline{T}_i(t)-\beta_i\overline{T}_{i+1}(t)=\overline{T}_i(t-\Delta t)+\Delta T_i(t) \qquad (10)$$

Terms involving $\overline{T}_0$ and $\overline{T}_{n+1}$ will be zero if we can assume that $\alpha_1=\beta_n=0$. Both assumptions can be well justified by assuming zero diffusion at the air-water interface ($K_1=0$), and zero bottom area in the lowermost layer ($A_{n+1}=0$). Introducing vector notation $\overline{T}(t)=\left[\overline{T}_1(t)\ldots\overline{T}_n(t)\right]^T$ makes it possible to write the implicit, finite-difference approximation of (4) as

$$F\,\overline{T}(t)=\overline{T}(t-\Delta t)+\Delta T(t) \qquad (11)$$

with *F* being a positive definite tridiagonal matrix given by

$$\begin{aligned} F_{i-1,i} &= -\alpha_i && i=2,\ldots,n \\ F_{i,i} &= 1+\alpha_i+\beta_i && i=1,\ldots,n \\ F_{i,i+1} &= -\beta_i && i=1,\ldots,n-1 \end{aligned} \qquad (12)$$

In other words, given the temperature distribution at the previous time step ($\overline{T}(t-\Delta t)$) and local heating over the last time step ($\Delta T(t)$), we can compute the present temperature distribution by solving the linear equation 11.

2.2 Calculation of the sediment-water heat flux

The calculation of the heat flux at the sediment-water interface is based on Fang and Stefan (1996). First the temperature profile is solved in a 10 m thick sediment layer using a similar implicit numerical method as with the lake water column (section 2.1). The vertical grid resolution Δz is 0.2 m in the 0-2 m sediment layer, and 0.5 m in the 2-10 m sediment layer. Heat diffusion coefficient K_{sed} is assumed constant with depth, and the variables α and β become in this case

$$\alpha_i=\frac{\Delta t}{\left(\Delta z_{up}\right)^2}K_{sed} \qquad (13a)$$

$$\beta_i = \frac{\Delta t}{(\Delta z_{down})^2} K_{sed} \qquad (13b)$$

where Δz_{up} and Δz_{down} are distances from the center of layer *i* to the centers of the layers above and below it. In addition we set temperature at the topmost sediment layer to be the same as the temperature in the water layer above it (values from previous time step are used in calculations)

$$\overline{T}_{sed\_1}(t) = \overline{T}_{water\_bot}(t - \Delta t) \qquad (14)$$

and assume that at ~10 m depth in the sediment, i.e. ~10 m below the lake bottom, the temperature becomes constant and heat flux vanishes, and we don't need to simulate the temperature evolution any deeper, i.e.

$$\frac{\partial \overline{T}_{sed\_n}}{\partial z} = 0 \qquad (15)$$

As in section 2.1, Terms involving $\overline{T}_{sed\_0}$ and $\overline{T}_{sed\_n+1}$ will be zero if we assume that $\alpha_1 = \beta_n = 0$. Furthermore, in order to keep the top sediment layer at the water bottom temperature, we set $\beta_1 = 0$. This means in practise that the temperature of the first sediment layer is known from water temperature (equation 14) and so we do not need to solve the diffusion equation for this layer.

As each water layer is in contact with the sediment, each water layer is associated with its own sediment column, and thus *n* (= total number of water layers) temperature profiles must be solved in the sediment per one model time step, which, of course, will increase the model runtime considerably (see section 5.4). The water-sediment interface (*WS*) area is approximated by the difference in horizontal area between two consecutive depth levels, $A_{WS\_i} = A_i - A_{i+1}$. The heat flux from sediment to water Q_{WS_i} [J d^{-1} m^{-2}] is

$$Q_{WS\_i} = K_{sed} \rho_{sed} c_{sed} \left. \frac{\partial T}{\partial z} \right|_{WS\_i} \qquad (16)$$

where K_{sed} (=0.035 m^2 d^{-1}) is the thermal diffusivity, ρ_{sed} (=2500 kg m^3) the density and c_{sed} (=1000 J kg^{-1} K^{-1}) the specific heat capacity of the sediment (Fang and Stefan, 1996). The temperature of the two uppermost sediment layers are used to approximate the temperature gradient at the sediment-water

interface. In MyLake model code Q_{WS_i} is further normalised so that its value is comparable to atmospheric and solar radiation heat fluxes (the normalised Q_{WS_i} can be applied over the whole top area of the water layer)

$$Q_{WS\_norm\_i} = Q_{WS\_i} \frac{A_{WS\_i}}{A_i} \tag{17}$$

2.3 Parameterisation of vertical diffusion and heat fluxes

The vertical diffusion coefficient K [m^2 d^{-1}] is estimated from the stability (Brunt-Väisälä) frequency $N^2 = \frac{g}{\rho_w}\frac{\partial \rho_w}{\partial z}$ [s^{-2}] (Hondzo and Stefan, 1993)

$$K = a_k (N^2)^{-0.43} \tag{18}$$

where a_k is parameterised by lake surface area A_s [km^2]. The default parameterisation, a_k = $0.00706(A_s)^{0.56}$ during ice-free period, is adopted from Hondzo and Stefan (1993) who used temperature profiles from Minnesota lake database to derive parameterisations for hypolimnetic eddy diffusivity. During ice covered period we use a default a_k = 0.000898, adopted from Fang and Stefan (1996). A minimum possible stability frequency N^2_{min} is defined (Hondzo and Stefan, 1993), which thus sets upper limit for K. A default value N^2_{min}=7.0×10^{-5} s^{-2} is adopted from Hondzo and Stefan (1993).

Local heating $\Delta T(t)$ during open water period is calculated for the surface layer by

$$\Delta T_1 = (Q_{WS\_norm\_1} + Q_{turb} + Q_{lw} + Q_{sw\_abs\_1}) A_1 / \rho_w C_p V_1 \tag{19a}$$

and for the subsurface layers by

$$\Delta T_{i>1} = (Q_{WS\_norm\_i} + Q_{sw\_abs\_i}) A_i / \rho_w C_p V_i \tag{19b}$$

where Q_{turb} is the turbulent heat flux (sensible and latent), Q_{lw} is the net longwave radiation flux, and $Q_{sw\_abs\_i}$ is the incoming solar radiation flux absorbed in the layer [J day^{-1} m^{-2}]. All fluxes are averages over a model time step, i.e. over a 24-hour period. In the ice-covered period only sediment-water heat flux and shortwave radiation penetrating through ice and snow contribute to local heating.

The light attenuation in water is divided into two wavelength bands, PAR light (photosynthetically active radiation; λ = 400-700 nm) and non-PAR light (λ < 400 or λ > 700 nm). Especially the longer wavelengths of the non-PAR light are rapidly attenuated in the near-surface layer. $Q_{sw\_abs\_i}$ is calculated by

$$Q_{sw\_abs\_i} = Q_{sw}(1-\alpha)\cdot \left\{ f_{PAR}\left[\exp(-\bar{\varepsilon}_{i-1} z_i) - \exp(-\bar{\varepsilon}_i z_{i+1}) \frac{A_{i+1}}{A_i} \right] + (1-f_{PAR})\cdot \left[\exp(-\bar{\hat{\varepsilon}}_{i-1} z_i) - \exp(-\bar{\hat{\varepsilon}}_i z_{i+1}) \frac{A_{i+1}}{A_i} \right] \right\} \quad (20)$$

where Q_{sw} is the incoming solar radiation flux at the surface, α is average daily albedo, f_{PAR} is the PAR fraction of the total shortwave energy, and $\bar{\varepsilon}_i$ and $\bar{\hat{\varepsilon}}_i$ the mean PAR and non-PAR light extinction coefficients down to the bottom of layer i (level z_{i+1}), respectively, taking into account both chlorophyll and non-chlorophyll related attenuation (see equation 43). The solar radiation that hits the bottom is assumed to be absorbed in the water layer and is taken into account in $Q_{sw\_abs\_i}$ by term A_{i+1}/A_i.

In the wintertime PAR light is first (strongly) attenuated in snow and ice layers before it reaches the water surface.

MyLake model code does not contain all functions for the calculation of the radiative and turbulent heat fluxes, surface wind stress or astronomical variables, but utilises the MATLAB *Air-Sea Toolbox* (http://sea-mat.whoi.edu/air_sea-html/). We refer thus to this toolbox for details on, e.g., the calculation of Q_{turb} and Q_{lw} Some shortwave radiation algorithms are, however, contained directly in MyLake code.

The albedos of melting ice and snow are taken as constants and given as model parameters. For lake water surface the average daily albedo is calculated as a function of sun height angle and total atmospheric transmissivity, using the MATLAB *Air-Sea Toolbox* (http://sea-mat.whoi.edu/air_sea-html/). If no observed global radiation data is given as input, the incoming shortwave radiation flux at the water or ice/snow surface (Q_{sw}) is calculated by

$$Q_{sw} = Q_0 f(N)\varphi(h) \quad (21)$$

where Q_0 is solar radiation flux outside the atmosphere, $\varphi(h)$ is the clear sky atmospheric transmissivity as a function of sun height angle at noon h ($\varphi(h)=0.377+0.00513h$ is determined from empirical data), and $f(N)$ is a cloud correction function of Reed (1977)

$$f(N) = 1 - 0.62N + 0.0019h \quad \text{, for } N \geq 0.3$$
$$f(N) = 1 \quad \text{, for } N < 0.3 \qquad (22)$$

where N is cloud fraction (decimal) and h is given in degrees.

2.4 Convective, wind-forced, and spring/autumn turnover mixing in the water column

Some processes in MyLake, such as daily wind stirring, water-ice heat flux and river inflow, are not solved simultaneously but in sequence. This means that in the model code they are applied to the lake system once in a day (e.g. at midnight).

Density is calculated by the IES80 algorithm (UNESCO, 1981) for temperatures above water freezing point. If supercooled water is encountered, ice formation is initiated instantly (see section 3.1). Convective mixing is induced by an unstable density profile. All groups of layers where the vertical density profile is unstable are thoroughly mixed with the first stable layer below the unstable layer(s) (i.e. a layer volume weighed mean temperature is calculated for the mixed water column). This procedure is continued until the vertical density profile in the whole water column becomes neutral or stable.

The total kinetic energy *TKE* [J] available for wind-induced mixing in open water period, accumulated over one model time step Δt (=86400 s) is calculated by

$$TKE = W_{str} A_s \sqrt{\frac{\tau^3}{\rho}} \Delta t \qquad (23)$$

where τ is wind stress [N m^{-2}] calculated from wind speed using the MATLAB *Air-Sea Toolbox* (http://sea-mat.whoi.edu/air_sea-html/), and W_{str} is a wind sheltering coefficient, for which a parameterisation by lake surface area A_s [km^2] is adopted from Hondzo and Stefan (1993; see section 2.3)

$$W_{str} = 1.0 - \exp(-0.3 A_s) \qquad (24)$$

In the ice covered period *TKE* is defined as zero (i.e., no wind-induced mixing occurs).

Wind-induced mixing in MyLake is handled in the following way (Ford and Stefan, 1980): first the thickess of the epilimnion layer z_{epi} is defined (epilimnion = the group of layers from surface

downwards with neutral vertical density profile). Then the *TKE* available (equation 23) is compared to the potential energy *PE* [J] needed to mix (i.e., lift) into the epilimnion the first layer below. If this layer has volume V_z, distance Δz_{M_z} from the layer's center of mass to the bottom of the epilimnion layer, and density difference $\Delta\rho_w$ compared to the density of the epilimnion, and the centre of mass of the epilimnion is at depth z_{M_epi} and V_{epi} is epilimnion volume, then the required mixing (i.e., lifting) energy is

$$PE = g\Delta\rho_w \frac{V_{epi}V_z}{V_{epi}+V_z}(z_{epi} + \Delta z_{M\_z} - z_{M\_epi}) \qquad (25)$$

If $TKE \geq PE$, then the first layer below the epilimnion is mixed thoroughly with the epilimnion layers, and the gained *PE* is subtracted from *TKE*. This procedure is continued with updated values of *TKE* and *PE* until the remaining *TKE* becomes smaller than the *PE* needed to mix a new layer into the epilimnion. The small remaining *TKE* is finally used to mix partially the next layer below the epilimnion with the epilimnion.

To ensure full turnover of the lake in spring and autumn, the temperature of the surface layer is not allowed to cross the temperature of the maximum density T_{maxrho} =3.98 °C until the whole water column has been cooled/warmed to T_{maxrho}. The procedure to handle this is following: whenever the calculated surface temperature would "leap" over T_{maxrho}, the temperature of the surface layer as well as all layers below it that have "leapt" over T_{maxrho}, are set to T_{maxrho}. In order to preserve energy, the "overshoot" energy of these layers E_{oversh} (i.e. the energy difference relative to T_{maxrho}) is used to cool/warm layers below the surface layer(s) to T_{maxrho} in autumn/spring. After this, the convective mixing will stabilise and mix the water column additionally. When the whole water column has become cooled/warmed to T_{maxrho}, then the remaining E_{oversh} is used to cool/warm the surface layer(s) additionally and the restriction of keeping the surface layer temperature at T_{maxrho} is relaxed. E_{oversh} is distributed exponentially in the water column (similarly as short-wave radiation) in the spring.

2.5 Addition of river inflow

River inflow is added to the top of the first water layer heavier than the inflow. The water column above the inflow level is then "lifted" according to the volume of the inflowing water. Moreover, the part of the water column that is "lifted" above the lake surface level (assumed to be invariant) is considered as the outflow and thus lost from the lake. However, if the inflow is lighter than the surface water layer, it is assumed to be mixed with the surface layer in proportion of the inflow and surface layer volumes.

3. Modelling of ice and snow cover

3.1 Growth of ice and snow layers

When water layer temperatures below freezing point are encountered, ice formation is triggered. The temperature of the supercooled layers is set to water freezing point T_f and the heat deficit relative to T_f is turned into an initial ice layer h_{ice} (by converting the sensible heat deficit in water into latent heat of ice). Whenever the air temperature T_a is below T_f, new ice thickness due to congelation ice growth is calculated from Stefan's law (Leppäranta, 1991)

$$h_{ice\_new} = \sqrt{h_{ice}^{\ 2} + \frac{2\kappa_{ice}}{\rho_{ice} L}(T_f - T_{ice})\Delta t} \tag{26}$$

where κ_{ice} [W K^{-1} m^{-1}] is the thermal conductivity of ice, ρ_{ice} [kg m^{-3}] the density of ice, and L the latent heat of freezing [J kg^{-1}]. The temperature of the ice surface T_{ice} is calculated by assuming that the heat fluxes through the ice and through the snow, or through the air layer if snow is absent, are equal at the ice/snow or ice/air interface, thus leading to

$$T_{ice} = \frac{pT_f + T_a}{1 + p} \tag{27}$$

where p=1/(10h_{ice}) in snow-free conditions, approximating somewhat warmer T_{ice} than T_a when the ice is still thin (Leppäranta, 1991). When a snow cover, with thickness h_s and thermal conductivity κ_s, exists on top of the ice, $p=\kappa_{ice}h_s/\kappa_s h_{ice}$ and T_{ice} is warmer than T_a due to the insulating effect of the snow cover. Thus, in the model p=max[$\kappa_{ice}h_s/\kappa_s h_{ice}$, 1/(10h_{ice})].

If the weight of the snow cover exceeds the buoyancy capacity of the ice layer, then water flooding on top of the ice can potentially occur (depending on the availability of waterways and on how well the isostatic balance between ice and water holds). The flooded water mixes with the lower part of the snow layer and forms a slush layer, which becomes snow ice when frozen (Saloranta, 2000). In MyLake snow ice formation is modelled by assuming that isostatic balance applies and that free waterways always exist for flooding. The water-soaked snow layer is assumed to be compacted directly to the density of ice, and hence turned into a snow ice layer (i.e. no water is frozen in modelled snow ice formation). The amount of new snow ice formation becomes then

$$\Delta h_{si} = \max\left[0, h_{ice}(\rho_{ice} / \rho_w - 1) + h_{s\_weq}\right] \quad (28)$$

where h_{s_weq} is the thickness of the snow layer in water equivalents. Snow ice is for simplicity assumed to have the same properties as congelation ice, and thus the newly formed ice in form of snow ice is subtracted from the snow layer and added to the ice layer. The amount of new snowfall (in water equivalents) is calculated from the daily precipitation data. The actual thickness of the snow layer (used e.g. in equation 27) is calculated by $h_s = h_{s\_weq}\ (\rho_w / \rho_s)$, where ρ_s is the bulk density of snow cover.

3.2 Melting of ice and snow layers, and snow compaction

Whenever the air temperature is above T_f, then T_{ice} is set to T_f, ice growth and snow fall processes are ceased and ice melting can occur. All snow must first melt before ice surface melting can start. The energy used for melting is calculated from the total heat flux at the surface assuming that the short-wave radiation, which is not reflected or penetrated to water column, is absorbed in the snow/ice layer. Albedo values of 0.77 and 0.3 are used as default for melting snow and ice surface, respectively (Perovich, 1998; Saloranta, 2000). If the snow layer is entirely melted during a time step, the remaining energy is used to melt the ice cover. Similarly, if the ice layer is entirely melted during a time step, the remaining energy is used to warm the water. This energy is distributed exponentially in the water column (similarly as short-wave radiation).

Whenever ice cover is present the temperature of the water surface layer is kept at T_f (i.e., we set $\beta_1 = 0$; equation 10, section 2.2). The heat flux at the ice-water interface, approximated using the temperature difference of the two topmost water layers, is used to melt ice at each time step. This heat flux thus lowers the ice growth rate somewhat or even causes melting at the bottom of the ice layer.

At the end of each time step the bulk snow density value ρ_s is updated. First a new, layer thickness weighed mean density is calculated from the densities of the old and new (i.e. new snowfall with density of 250 kg m^{-3}) snow layers. When $T_a < T_f$ further density increase owing to compaction, is calculated by using the formula by Yen (1981) and calculating compaction in the middle of the snow layer:

$$\Delta\rho_s = C_1 \rho_s \frac{h_{s\_weq}}{2} \cdot \exp(-C_2 \rho_s) \cdot \exp\left[-0.08\left(T_f - \frac{T_{ice} + T_a}{2}\right)\right] \cdot \Delta t \quad (29)$$

where C_1 and C_2 are empirical coefficients (7.0 m^{-1}h^{-1} and 0.021 m^{3}kg^{-1}, respectively; Yen, 1981; Saloranta, 2000). If $T_a \geq T_f$ snow bulk density is set to a maximum value ρ_{s_max} = 450 kg m^{-3}.

4. Modelling of dissolved and particulate matter and phytoplankton

4.1 General model for dissolved and particulate matter

In order to represent vertical movements of e.g. phytoplankton or sedimentating particles, an advective term $A\partial(wC)/\partial z$ must be added to the diffusive equation (equation 1). The advective-diffusive equation thus becomes:

$$A\frac{\partial C}{\partial t} = \frac{\partial}{\partial z}\left[KA\frac{\partial C}{\partial z}\right] - A\frac{\partial (wC)}{\partial z} + AS \qquad (30)$$

where C is an arbitrary state variable (e.g. concentration of chlorophyll *a*; used in place of T in equation 1), w is the downward vertical velocity and S is a source/sink term. Note that not taking partial derivative of A in the advection term means that when sedimenting particles reach the bottom (at any depth level) they will stay there (until resuspended later). Thus no direct ”funnelling effect”, i.e. accumulation of suspended particles towards the bottom of the lake ”cone”, is allowed. The numerical approximation for equation 30 is a hybrid exponential difference method described in Dhamotharan et al. (1981). This hybrid method assumes a constant settling velocity w, and weights the central and upwind numerical schemes differently depending on the grid Peclet number $Pe=w\Delta z/K$. At large Pe values advection dominates and the upwind difference scheme (i.e. evaluating the derivatives at grid points i-1 and i in case of positive w) should be used, and at small Pe values diffusion dominates and the central difference scheme (i.e. evaluating the derivatives at grid points i-1, i and i+1) should be used, in order to reduce the errors and distortion in the advective-diffusive numerical scheme (for detailed error analysis, see Dhamotharan et al. (1981)).

When applied to our numerical grid the hybrid exponential numeric scheme for solving equation 30 becomes in its fully implicit form

$$\frac{\overline{C}_i(t) - \overline{C}_i(t-\Delta t)}{\Delta t} = \frac{w}{\Delta z}\left[\overline{C}_{i-1}(t) + \frac{\overline{C}_{i-1}(t) - \overline{C}_i(t)}{\exp(Pe_i) - 1} - \overline{C}_i(t) - \frac{\overline{C}_i(t) - \overline{C}_{i+1}(t)}{\exp(Pe_{i+1}) - 1}\right] \qquad (31)$$

By rearranging equation 31 so that all terms involving $\overline{C}(t)$ appear on the left-hand side (as with equation 10), this gives

$$-\alpha_i \overline{C}_{i-1}(t) + \gamma_i \overline{C}_i(t) - \beta_i \overline{C}_{i+1}(t) = \overline{C}_i(t - \Delta t) + \Delta \overline{C}_i(t) \quad (32)$$

where

$$\alpha_i = \frac{w\Delta t}{\Delta z}\left[1 + \left(\frac{1}{\exp(Pe_i) - 1}\right)\right] \quad (33a)$$

$$\beta_i = \frac{w\Delta t}{\Delta z}\left(\frac{1}{\exp(Pe_{i+1}) - 1}\right) \quad (33b)$$

$$\gamma_i = 1 + \alpha_i + \beta_i \quad (33c)$$

$$Pe_i = \frac{wV_i}{K_i A_i} \quad (33d)$$

$$Pe_{i+1} = \frac{wV_i}{K_{i+1} A_{i+1}} \quad (33e)$$

The coefficients in equation 32 can be arranged in the tridiagonal matrix form and the system of equations solved as described in section 2.1.

The boundary condition at the surface (i=1) is no net transfer, thus the two first terms in the brackets in equation 31 cancel each other giving coefficient values

$$\alpha_1 = 0 \quad (34a)$$

$$\gamma_1 = 1 + \beta_1 + \frac{w\Delta t}{\Delta z} \quad (34b)$$

The boundary condition at the bottom (i=n) is no diffusion, and thus the concentration gradient between layers n and $n+1$, where $n+1$ denotes an imagined "dummy" layer, is thought to vanish so that $\overline{C}_n = \overline{C}_{n+1}$, giving coefficient values

$$\gamma_n = 1 + \alpha_n \quad (34c)$$

$$\beta_n = 0 \quad (34d)$$

Note that in MyLake the resuspension of particulate matter from sediment is added to the water column via the source term S of the advective-diffusive equation (see section 4.2).

4.2 A simple, vertically structured phytoplankton model

The phytoplankton model has only two state variables – phytoplankton biomass C [mg m^{-3} = µg l^{-1}] measured as chlorophyll *a* and dissolved inorganic phosphorus (phosphate) P [mg m^{-3} = µg l^{-1}]. For simplicity, we assume that phytoplankton has fixed composition, so that P and C will be related by a constant stoichiometric yield coefficient y_c. If phytoplankton have Redfield composition (C:P = 106 by atoms, 40 by weight) and a carbon to chlorophyll ratio of similar magnitude, then the yield coefficient y_c will be approximately unity.

The main differences between the two state variables are that chlorophyll (C) is subject to sinking losses and attenuates light, while phosphate (P) does neither. The one-dimensional partial differential equations for P and C can thus be written:

$$\begin{aligned} A\frac{\partial P}{\partial t} &= \frac{\partial}{\partial z}\left[KA\frac{\partial P}{\partial z}\right] - Ay_c^{-1}rC \\ A\frac{\partial C}{\partial t} &= \frac{\partial}{\partial z}\left[KA\frac{\partial C}{\partial z}\right] - A\frac{\partial (wC)}{\partial z} + A(rC + S_{Csed}) \end{aligned} \qquad (35)$$

where w is the sinking velocity of chlorophyll (typical value 0.1-1 m d^{-1}), and S_{Csed} [mg m^{-3} d^{-1}] is the resuspension rate of C from the sediment (this source can e.g. be used to ensure some background concentration of C in the water column after a long ice-covered winter season). The resuspension rate for layer i is calculated by

$$S_{Csed\_i} = \frac{A_{WS\_i} S_{Csedflux\_i}}{V_i} \qquad (36)$$

where A_{WS} is the water-sediment interface (WS) area, and $S_{Csedflux}$ flux [mg m^{-2} d^{-1}] is the resuspension.

The resuspension of C (and particulate phosphorus, PP, see section 4.3) is thought to be due to mechanical sediment perturbation. Therefore, resuspension is restricted to the water layers above the depth of the pycnocline z_{PC}, where the strongest turbulence levels are expected. Pycnocline depth is calculated by

$$z_{PC} = \frac{\sum_k D_k z_k}{\sum_k D_k} \qquad (37)$$

where

$$\begin{cases} D_k = 0 & \text{if } \left|\frac{\Delta\rho_k}{\Delta z}\right| < 0.1 \text{ kg m}^{-3}/\text{m} \\ D_k = \left|\frac{\Delta\rho_k}{\Delta z}\right| & \text{if } \left|\frac{\Delta\rho_k}{\Delta z}\right| \geq 0.1 \text{ kg m}^{-3}/\text{m} \end{cases} \quad (38)$$

If the density difference between two consecutive layers does not exceed the threshold limit of 0.1 kg m^{-3}/m, then the interface between these layers is not taken into account in calculation of the pycnocline depth. Furthermore, if none of the density differences between the layers exceed the threshold limit of 0.1 kg m^{-3}/m, then z_{PC} is not defined at all. In this case resuspension is allowed from top to bottom in the open water season. In ice covered conditions no resuspension from sediment is allowed, neither for *C* or *PP*.

The daily amount of resuspension is subtracted from the sediment "*C*-store", and it cannot exceed the amount of *C* stored in the sediment. Sedimentation of *C* contributes to filling this "*C*-store", while transformation to particulate phosphorus (section 4.3) and resuspension contribute to emptying it. Note that the handling of river inflow-outflow dynamics is not included in equation 35, but that this is handled separately (see section 2.4).

All biological processes in this model are contained in r [d^{-1}], the net, specific rate of change in chlorophyll concentration. The net rate of change can be decomposed into the difference between specific growth and loss rates, i.e. $r = \mu - m$. All local loss processes due to respiration, lysis, predation, parasitism, etc. are aggregated into a single first-order remineralisation process. Direct conversion of chlorophyll losses into phosphate gains, through a constant yield coefficient, implies that we deliberately ignore the possibility of P-containing organic detritus as an intermediate in the remineralisation process. Remineralisation is assumed to be an exponential function of temperature T [°C]

$$m = m(20)\theta^{T-20} \quad (39)$$

where *m(20)* is the rate in a reference temperature (20 °C), with typical value around 0.2 d^{-1}. If we assume that biological rates typically double on a 10 °C temperature increase (i.e. Q_{10} = 2), then θ = $\exp(10^{-1}\ln 2) \approx 1.072$.

The specific growth rate μ will typically be a function of phosphate concentration, temperature, and light. Since we assume constant chlorophyll yield per unit phosphorus there is no need to employ

a more sophisticated representation of nutrient limited growth than the Monod model. When light is non-limiting, then growth is a saturation function (a rectangular hyperbola) of phosphate concentration

$$\mu = \mu'(T)\frac{P}{P' + P} \tag{40}$$

where $\mu'(T)$ is the maximal attainable growth rate, when neither light nor phosphate are limiting, having the same type of exponential temperature dependence as remineralisation, i.e.

$$\mu(T) = \mu(20)\theta^{T-20} \tag{41}$$

The half-saturation parameter P' of the Monod model will typically be less than 1 µg P / l, while the maximal specific growth rate at 20 °C, $\mu(20)$, will be in the range 1 - 1.5 d^{-1}.

Before we can deal with light-limited growth we have to go into some details about the vertical light gradient. Since chlorophyll may vary with depth, and since chlorophyll may contribute strongly to light absorption, we may no longer assume that light attenuation follows a Beer-Lambert law with a constant attenuation coefficient. Instead we will assume that the PAR attenuation coefficient ε is a function of depth and that the following integral relation holds

$$I_z = I_0 \exp\left(-\int_0^z \varepsilon(x)\,dx\right) = I_0 \exp\left(-\overline{\varepsilon}_z z\right) \tag{42}$$

where I_0 and I_z [mol quanta m^{-2} s^{-1}] are the PAR irradiances at surface and at depth z, and where the latter identity comes from the mean value theorem of calculus ($\overline{\varepsilon}_z$ is the depth average of $\varepsilon(x)$ for $0 \le x \le z$). If light attenuation is a linear function of chlorophyll concentration then by linearity of the integral operator, the mean attenuation coefficient also becomes a linear function of the mean chlorophyll concentration

$$\overline{\varepsilon}_z = \varepsilon_0 + \beta \overline{C}_z \tag{43}$$

where ε_0 is the non-chlorophyll related light attenuation, β is the optical cross section of chlorophyll (m^2 mg^{-1}), and $\overline{C}_z$ is the mean chlorophyll concentration from the surface to depth *z*. In MyLake,

values of C_z from previous timestep are used to calculate $\bar{\varepsilon}_z$. The median value of β in table 9.1 of Kirk (1983) is 0.015 m^2 mg^{-1}, while the background attenuation can vary from 0.08-2.0 m^{-1} (ε_0 for pure water is 0.03-0.06 m^{-1}, depending on wavelength).

If we assume a total-absorbing mixed layer of depth z, then the average light and nutrient limited net, specific rate of change in this layer can be written as

$$\bar{r}_z = \bar{\mu}_z \frac{\lambda}{\bar{\varepsilon}_z z} H\left(\frac{I'_0}{I'}\right) - \bar{m}_z \tag{44}$$

where $\bar{\mu}_z$, $\bar{m}_z$, and $\bar{\varepsilon}_z$ are the depth-averaged versions of μ, m and ε, λ is the fractional day length (dimensionless, computable from standard astronomical formulae for a given latitude and time of year), and $I'_0 / I' \equiv u$ is the scaled surface irradiance at noon. The scaling parameter, I', also called the light saturation level of photosynthesis, typically has values around 10 mol quanta m^{-2} d^{-1} (= 116 µmol quanta m^{-2} s^{-1}). The light limitation function H is

$$H(u) = \begin{cases} \frac{2}{3}u & u \le 1 \\ \frac{2}{3}u + \ln\frac{\sqrt{u}+\sqrt{u-1}}{\sqrt{u}-\sqrt{u-1}} - \frac{2}{3}(u+2)\frac{\sqrt{u-1}}{\sqrt{u}} & u > 1 \end{cases} \tag{45}$$

Full derivation of *H(u)* is given in Appendix A.

Recalling from section 2.1, in a control volume discretization of the (partial differential) model equations we will be concerned with a series of vertical layers (Figure 1) labelled such that layer i (i = 1..n) extends from depth z_i to z_{i+1} (the upper limit z_1 of the upper layer is always zero, the thickness of a given layer is $\Delta z_i = z_{i+1} - z_i$). When given T_i, P_i, C_i – water temperature and model state variables in layer i, we can compute μ_i, m_i, and ε_i - the local values of light unlimited growth rate, remineralisation rate, and attenuation coefficient for layer i. From ε_i, we can also compute $\bar{\varepsilon}_i = z_i^{-1} \sum_{j=1}^{i} \Delta z_j \, \varepsilon_j$, the average attenuation coefficient down to the bottom of layer i, from which we then can compute the PAR irradiance at noon at the depth level z_i as $I'_{zi} = I'_0 \exp(-\bar{\varepsilon}_{i-1} z_i)$. Finally, this leads us to the expression for the net, specific rate of change in a given layer

$$r_i = \mu_i \frac{\lambda}{\varepsilon_i \Delta z_i}\left[H\left(\frac{I_{zi}^{'}}{I^{'}}\right) - H\left(\frac{I_{zi+1}^{'}}{I^{'}}\right)\right] - m_i \qquad (46)$$

Surface irradiance at noon will typically be computed from short-wave energy flux Q_{sw} [W m^{-2}], which will be needed anyway for local heating term in the physical lake model (section 2.3), and from the model curve used for representing surface irradiance as function of time of day. Short-wave flux and photosynthetically active radiation (PAR, 400-700 nm) are related through the PAR fraction of total short-wave energy (f_{PAR}, typically 42-48%) and the average energy of PAR photons (E_{PAR}, 240800 J mol^{-1}):

$$f_{PAR} Q_{sw} = E_{PAR} I_0^{'} \int_{-\lambda/2}^{\lambda/2} G(2t/\lambda)dt \qquad (47)$$

where *G(x)* is a symmetrical function described in Appendix A. For the inverted parabola used in the analytical model of integrated photosynthesis, this relationship becomes

$$I_0^{'} = \frac{3}{2}\frac{f_{PAR} Q_{sw}}{\lambda} E_{PAR}^{-1} \qquad (48)$$

For the commonly used cosine model for irradiance as function of time of day, the relationship between integral and peak irradiance will be very similar, but with the factor $3/2$ replaced by $\pi/2$.

4.3 Modelling of particulate phosphorus and tracers

Phosphorus absorbed to suspended particles (particulate phosphorus, *PP*) is the other phosphorus state variable in MyLake. *PP* is both sedimented and resuspended from the sediment, in a similar way as chlorophyll *a* (section 4.2). While suspended in the water column, the transformation from *PP* to phosphate *P* is formulated as

$$\left.\frac{\partial P}{\partial t}\right|_{PP} = k(T)_{PP} PP \qquad (49)$$

where $k(T)_{PP}$ is the transformation rate coefficient [d^{-1}] having a temperature dependence similar to that described in equations 39 and 41

$$k(T)_{PP} = k(20)_{PP}\theta^{T-20} \quad (50)$$

PP storage in the sediment is monitored in a "*PP*-store", similarly as chlorophyll *a* (see section 4.2). The transformation of chlorophyll *a* to *PP* in the sediment is modelled using the same type of exponential decay and temperature dependent transformation rate as in equations 49 and 50 above. Figure 2 shows the possible flows of *P*, *PP* and *C* in MyLake model.

Also two passive tracers, one dissolved and one particulate, are included as model state variables. As these tracer do not take part in any reactions they can be used to test and monitor the functioning of the transfer processes in the model, i.e. settling, mixing and and river inflow. Real-life examples of such tracers could be salinity (dissolved) and clay particles (sedimenting).

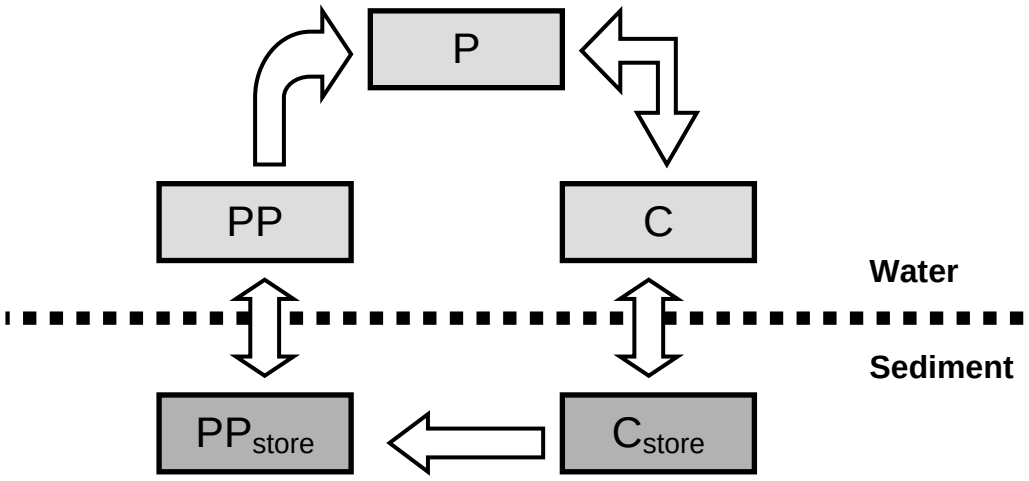

Figure 2. *A schematic illustration of the flows between the three state variables in MyLake model, dissolved inorganic phosphorus (phosphate, P), particulate phosphorus (PP), and chlorophyll a (C). PP_{store} and C_{store} denote the stores of particulate phosphorus and chlorophyll a in the sediment, respectively.*

5. Running a MyLake model application

5.1 General features

The MyLake model code consists of five modules (MATLAB scripts, ”m-files”):

solvemodel_v11.m	Contains most of the model algorithms and numerical solving of the equations. Contains also a number of ”switches” with which particular processes can be disabled in the model code (section 5.3);
heatflux_v11.m	Handles calculation of turbulent and radiative heat fluxes, and other physical and astronomical variables. Utilises MATLAB *Air-Sea Toolbox* (by Rich Pawlowicz, Woods Hole: http://sea-mat.whoi.edu/air_sea-html/);
sedimentheat_v11.m	Calculates the heat diffusion in sediment;
IOflow_v11.m	Handles the addition of river inflow;
modelinputs_v11.m	Handles the reading of input data, initial conditions and parameters from the three Excel files described in sections 5.2.1.-5.2.3.

5.2 Parameter and input file structures

In addition to the model code (including the *Air-Sea Toolbox*), three different parameter and input data files are required to run a MyLake model application. These three files contain 1) time series of meteorological variables and inflow properties, 2) lake morphometry and initial profiles, and 3) model parameter values. These files are formatted in Excel spreadsheet software. File formats and required units (the latter are given in square brackets) are explained below (sections 5.2.1-5.2.3) and file templates are shown in Figures 3-5. Note that the first cell in the upper left corner (A1) must contain a dummy number (e.g. -999) so that MATLAB reads in the columns and rows correctly.

5.2.1 Meteorological and inflow time series

Note that time series with daily resolution are required, and that values for missing observations or measurement dates in the meteorological and inflow time series are in MyLake automatically estimated by linear interpolation.

Rows

1-2: Header rows

(**Important!** The first cell on the first row (A1) must contain a number, e.g –999)

3-end: Data rows

Columns

1. Year
2. Month
3. Day
4. Global radiation [MJ m^{-2} day^{-1}]
5. Cloud cover (0-1)
6. Air temperature at 2 meter height [°C]
7. Relative humidity at 2 meter height [%]
8. Air pressure at station level [hPa]
9. Wind speed at 10 m height [m s^{-1}]
10. Precipitation [mm d^{-1}]
11. Inflow volume [m^3 d^{-1}]
12. Inflow temperature [°C]; if ”NaN” (“Not a Number”, a MATLAB expression for missing value) then the inflow is assumed to mix with the surface layer
13. Inflow concentration of the passive tracer [-]
14. Inflow concentration of the passive sedimenting tracer [-]
15. Inflow concentration dissolved inorganic phosphorus (phosphate) [µg l^{-1} = mg m^{-3}]
16. Inflow concentration of chlorophyll *a* [µg l^{-1} = mg m^{-3}]
17. Inflow concentration of particulate phosphorus [µg l^{-1} = mg m^{-3}]

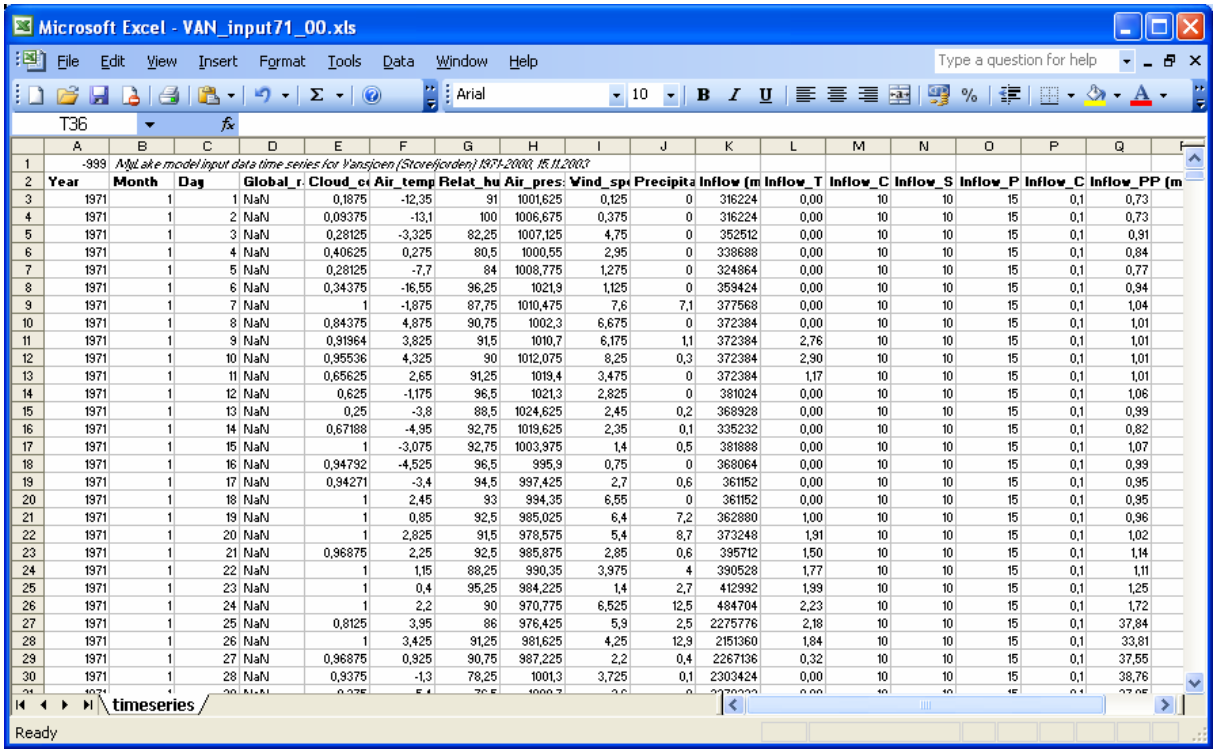

	A	B	C	D	E	F	G	H	I	J	K	L	M	N	O	P	Q
1	-999	MyLake model input data time series for Vansjoen (Storefjorden) 1971-2000, 15.11.2003															
2	Year	Month	Day	Global_r	Cloud_c	Air_temp	Relat_hu	Air_pres	Wind_sp	Precipita	Inflow (m	Inflow_T	Inflow_C	Inflow_S	Inflow_P	Inflow_C	Inflow_PP (m
3	1971	1	1	NaN	0,1875	-12,35	91	1001,625	0,125	0	316224	0,00	10	10	15	0,1	0,73
4	1971	1	2	NaN	0,09375	-13,1	100	1006,675	0,375	0	316224	0,00	10	10	15	0,1	0,73
5	1971	1	3	NaN	0,28125	-3,325	82,25	1007,125	4,75	0	352512	0,00	10	10	15	0,1	0,91
6	1971	1	4	NaN	0,40625	0,275	80,5	1000,55	2,95	0	338688	0,00	10	10	15	0,1	0,84
7	1971	1	5	NaN	0,28125	-7,7	84	1008,775	1,275	0	324864	0,00	10	10	15	0,1	0,77
8	1971	1	6	NaN	0,34375	-16,55	96,25	1021,9	1,125	0	359424	0,00	10	10	15	0,1	0,94
9	1971	1	7	NaN	1	-1,875	87,75	1010,475	7,6	7,1	377568	0,00	10	10	15	0,1	1,04
10	1971	1	8	NaN	0,84375	4,875	90,75	1002,3	6,675	0	372384	0,00	10	10	15	0,1	1,01
11	1971	1	9	NaN	0,91964	3,825	91,5	1010,7	6,175	1,1	372384	2,76	10	10	15	0,1	1,01
12	1971	1	10	NaN	0,95536	4,325	90	1012,075	8,25	0,3	372384	2,90	10	10	15	0,1	1,01
13	1971	1	11	NaN	0,65625	2,65	91,25	1019,4	3,475	0	372384	1,17	10	10	15	0,1	1,01
14	1971	1	12	NaN	0,625	-1,175	96,5	1021,3	2,825	0	381024	0,00	10	10	15	0,1	1,06
15	1971	1	13	NaN	0,25	-3,8	88,5	1024,625	2,45	0,2	368928	0,00	10	10	15	0,1	0,99
16	1971	1	14	NaN	0,67188	-4,95	92,75	1019,625	2,35	0,1	335232	0,00	10	10	15	0,1	0,82
17	1971	1	15	NaN	1	-3,075	92,75	1003,975	1,4	0,5	381888	0,00	10	10	15	0,1	1,07
18	1971	1	16	NaN	0,94792	-4,525	96,5	995,9	0,75	0	368064	0,00	10	10	15	0,1	0,99
19	1971	1	17	NaN	0,94271	-3,4	94,5	997,425	2,7	0,6	361152	0,00	10	10	15	0,1	0,95
20	1971	1	18	NaN	1	2,45	93	994,35	6,55	0	361152	0,00	10	10	15	0,1	0,95
21	1971	1	19	NaN	1	0,85	92,5	985,025	6,4	7,2	362880	1,00	10	10	15	0,1	0,96
22	1971	1	20	NaN	1	2,825	91,5	978,575	5,4	8,7	373248	1,91	10	10	15	0,1	1,02
23	1971	1	21	NaN	0,96875	2,25	92,5	985,875	2,85	0,6	395712	1,50	10	10	15	0,1	1,14
24	1971	1	22	NaN	1	1,15	88,25	990,35	3,975	4	390528	1,77	10	10	15	0,1	1,11
25	1971	1	23	NaN	1	0,4	95,25	984,225	1,4	2,7	412992	1,99	10	10	15	0,1	1,25
26	1971	1	24	NaN	1	2,2	90	970,775	6,525	12,5	484704	2,23	10	10	15	0,1	1,72
27	1971	1	25	NaN	0,8125	3,95	86	976,425	5,9	2,5	2275776	2,18	10	10	15	0,1	37,84
28	1971	1	26	NaN	1	3,425	91,25	981,625	4,25	12,9	2151360	1,84	10	10	15	0,1	33,81
29	1971	1	27	NaN	0,96875	0,925	90,75	987,225	2,2	0,4	2267136	0,32	10	10	15	0,1	37,55
30	1971	1	28	NaN	0,9375	-1,3	78,25	1001,3	3,725	0,1	2303424	0,00	10	10	15	0,1	38,76

Figure 3. *Example of a MyLake input forcing data file.*

5.2.2 Bathymetry and initial profiles

Note that linear temperature profile between the lake water temperature and 4 °C is initially assumed in the sediment columns.

Rows

1-2: Header rows

(**Important!** The first cell on the first row (A1) must contain a number, e.g –999)

3-end: Data rows

Columns

1. Depth levels (meters from surface; positive values); the first and last levels must be zero and the maximum depth, respectively

(*the following variable values must be given at all depth levels of column 1*)

2. Horizontal areas [m^2]; the first and last levels must be lake surface area and zero, respectively
3. Initial profile of temperature [°C]
4. Initial profile of the passive tracer [-]
5. Initial profile of the passive sedimenting tracer [-]
6. Initial profile of dissolved inorganic phosphorus (phosphate) [$\mu g\ l^{-1} = mg\ m^{-3}$]
7. Initial profile of chlorophyll *a* [$\mu g\ l^{-1} = mg\ m^{-3}$]
8. Initial profile of particulate phosphorus [$\mu g\ l^{-1} = mg\ m^{-3}$]
9. Initial profile of sediment store of chlorophyll *a* [$mg\ m^{-2}$]
10. Initial profile of sediment store of particulate phosphorus [$mg\ m^{-2}$]
11. Initial value of total ice thickness [m]
12. Initial value of snow thickness [m]

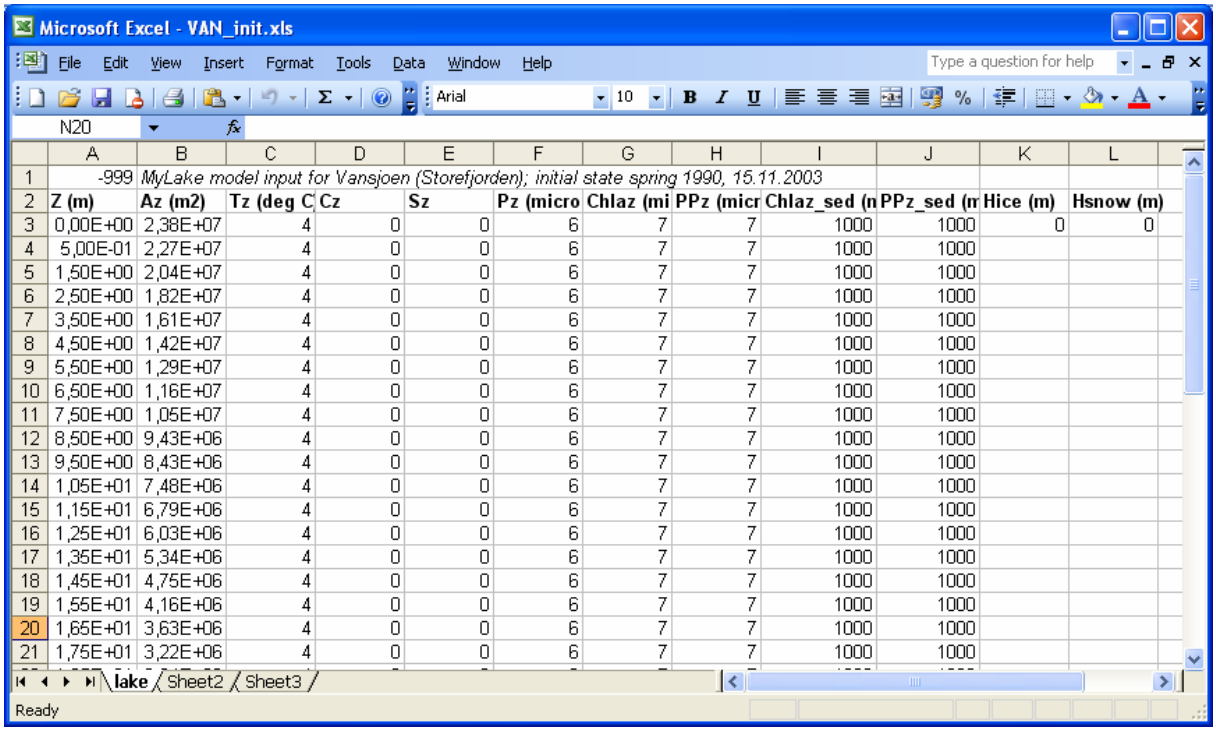

Microsoft Excel - VAN_init.xls

File Edit View Insert Format Tools Data Window Help

	A	B	C	D	E	F	G	H	I	J	K	L
1	-999	*MyLake model input for Vansjoen (Storefjorden); initial state spring 1990, 15.11.2003*										
2	**Z (m)**	**Az (m2)**	**Tz (deg C**	**Cz**	**Sz**	**Pz (micro**	**Chlaz (mi**	**PPz (micr**	**Chlaz_sed (n**	**PPz_sed (n**	**Hice (m)**	**Hsnow (m)**
3	0,00E+00	2,38E+07	4	0	0	6	7	7	1000	1000	0	0
4	5,00E-01	2,27E+07	4	0	0	6	7	7	1000	1000		
5	1,50E+00	2,04E+07	4	0	0	6	7	7	1000	1000		
6	2,50E+00	1,82E+07	4	0	0	6	7	7	1000	1000		
7	3,50E+00	1,61E+07	4	0	0	6	7	7	1000	1000		
8	4,50E+00	1,42E+07	4	0	0	6	7	7	1000	1000		
9	5,50E+00	1,29E+07	4	0	0	6	7	7	1000	1000		
10	6,50E+00	1,16E+07	4	0	0	6	7	7	1000	1000		
11	7,50E+00	1,05E+07	4	0	0	6	7	7	1000	1000		
12	8,50E+00	9,43E+06	4	0	0	6	7	7	1000	1000		
13	9,50E+00	8,43E+06	4	0	0	6	7	7	1000	1000		
14	1,05E+01	7,48E+06	4	0	0	6	7	7	1000	1000		
15	1,15E+01	6,79E+06	4	0	0	6	7	7	1000	1000		
16	1,25E+01	6,03E+06	4	0	0	6	7	7	1000	1000		
17	1,35E+01	5,34E+06	4	0	0	6	7	7	1000	1000		
18	1,45E+01	4,75E+06	4	0	0	6	7	7	1000	1000		
19	1,55E+01	4,16E+06	4	0	0	6	7	7	1000	1000		
20	1,65E+01	3,63E+06	4	0	0	6	7	7	1000	1000		
21	1,75E+01	3,22E+06	4	0	0	6	7	7	1000	1000		

lake Sheet2 Sheet3

Ready

Figure 4. *Example of a MyLake morphometry and initial profile file.*

5.2.3 Model parameters

Rows

1. Header row

   (**Important!** The first cell on the first row (A1) must contain a number, e.g –999)
2. Header row
3. *dz* [m], model vertical grid step (i.e., model layer thickness)
4. a_k [-] (equation 18), diffusion parameter during open water periods; if ”NaN” then a_k is calculated from lake surface area (page 13)
5. a_k [-] (equation 18), diffusion parameter during lake ice periods; if ”NaN” then a_k is calculated from lake surface area (page 13)
6. N^2_{min} [s^{-2}] (page 13); if ”NaN” then a default value $7x10^{-5}$ is assumed (page 13)
7. W_{str} [-] (equations 23, 24); if “NaN” then W_{str} is calculated from lake surface area (eq. 24)
8. $\hat{\varepsilon}_0$ [m^{-1}] (equations 20, 43), non-PAR light extinction coefficient for water (non-chlorophyll related)
9. ε_0 [m^{-1}] (equations 20, 43), PAR light extinction coefficient for water (non-chlorophyll related)
10. Lake latitude [decimal degrees]
11. Lake longitude [decimal degrees]

12. w [m d^{-1}] (equation 30), for sedimenting passive tracer; must be *w>0*
13. w [m d^{-1}] (equation 30), for chlorophyll *a*; must be *w>0*
14. w [m d^{-1}] (equation 30), for particulate phosphorus; must be *w>0*
15. α_{ice} [-], melting ice albedo (page 17)
16. α_{snow} [-], melting snow albedo (page 17)
17. *I_scV* [-], dimensionless scaling factor for inflow volume
18. *I_scT* [°C], scaling coefficient for inflow temperature
19. *I_scC* [-], dimensionless scaling factor for inflow concentration of passive tracer
20. *I_scS* [-], dimensionless scaling factor for inflow concentration of passive sedimenting tracer
21. *I_scP* [-], dimensionless scaling factor for inflow concentration of dissolved inorganic phosphorus (phosphate)
22. *I_scChl* [-], dimensionless scaling factor for inflow concentration of chlorophyll *a*
23. *I_scPP* [-], dimensionless scaling factor for inflow concentration of particulate phosphorus
24. y_c [-], (page 20)
25. *m(20)* [d^{-1}] (equation 39)
26. $\mu(20)$ [d^{-1}] (equation 41)
27. $k(20)_{PP}$ [d^{-1}] (equation 50)
28. $m(20)_{sed}$ [d^{-1}], chlorophyll *a* to particulate phosphorus transformation rate in the sediment store at 20 °C (page 25)
29. *P'* [µg l^{-1} = mg m^{-3}] (equation 40)
30. *I'* [mol (quanta) m^{-2} s^{-1}] (equation 44)
31. f_{PAR} [-] (equation 47)
32. β [m^2 mg^{-1}] (equation 43)
33. λ_{ice} [m^{-1}], PAR light attenuation coefficient for ice
34. λ_{snow} [m^{-1}], PAR light attenuation coefficient for snow
35. $S_{Csedflux}$ [mg m^{-2} d^{-1}] (equation 36), chlorophyll *a* resuspension rate
36. $S_{PPsedflux}$ [mg m^{-2} d^{-1}], particulate phosphorus resuspension rate, see page 25)

Columns (from 3rd row)

1. Parameter names (optional; used in connection with e.g. plotting of figures)
2. Nominal parameter values
3. Minimum of the parameter value range (optional for normal single model runs, but at least one dummy value (e.g. -9) must be given so that MATLAB can read the file in correctly)
4. Maximum of the parameter value range (optional for normal single model runs, but at least one dummy value (e.g. -9) must be given so that MATLAB can read the file in correctly)

5. Remarks (optional). In the example of Figure 5 this column is used to denote the units in which parameter values are required by MyLake model code (fixed units, see list above). This is highly recommended.
6. Remarks (optional). In the example of Figure 5 this column is used to explain the parameter symbols.

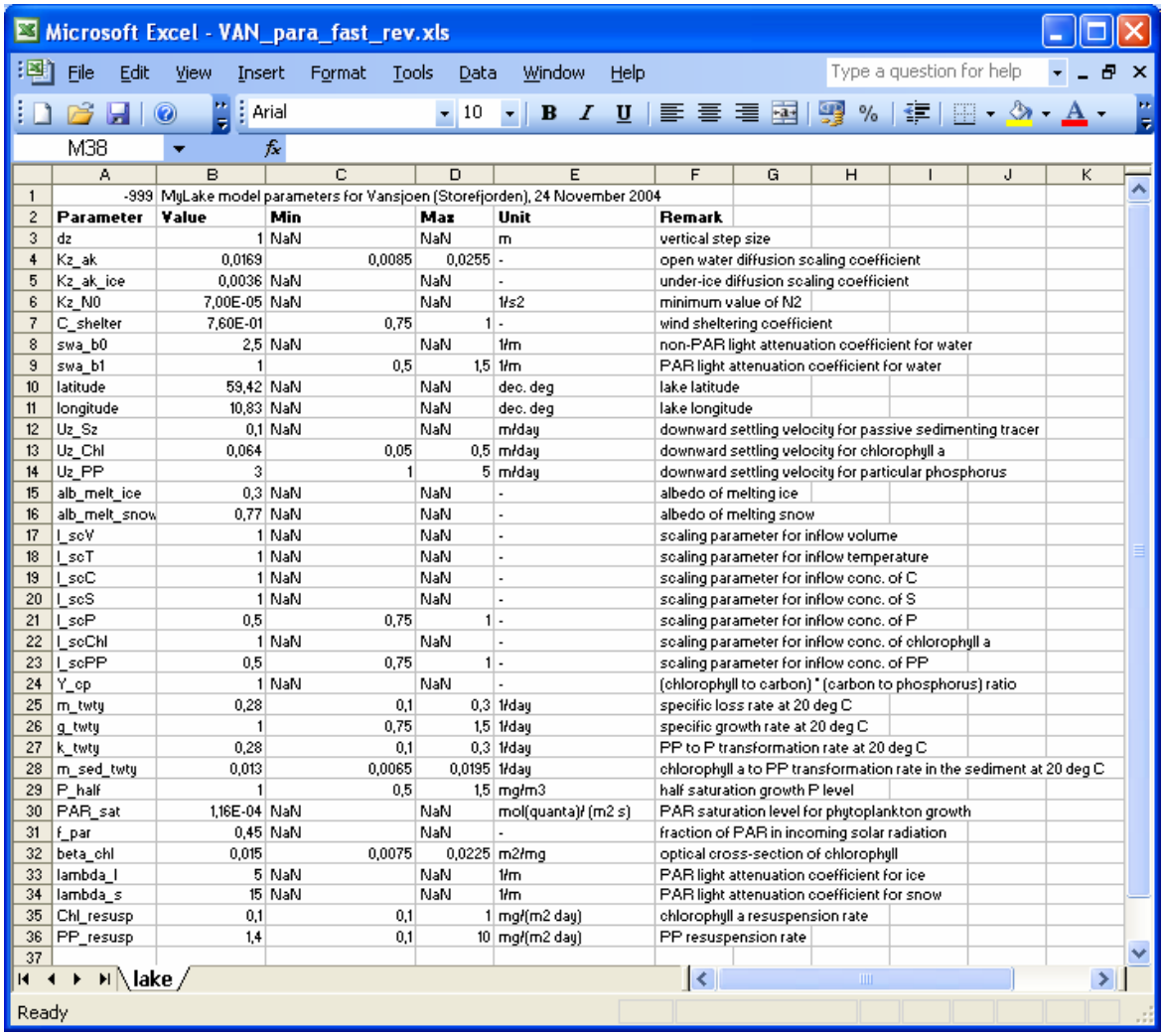

Microsoft Excel - VAN_para_fast_rev.xls

File Edit View Insert Format Tools Data Window Help — Type a question for help

Arial 10 B I U

M38

	A	B	C	D	E	F	G	H	I	J	K
1	-999	MyLake model parameters for Vansjoen (Storefjorden), 24 November 2004									
2	**Parameter**	**Value**	**Min**	**Max**	**Unit**	**Remark**					
3	dz	1	NaN	NaN	m	vertical step size					
4	Kz_ak	0,0169	0,0085	0,0255	-	open water diffusion scaling coefficient					
5	Kz_ak_ice	0,0036	NaN	NaN	-	under-ice diffusion scaling coefficient					
6	Kz_N0	7,00E-05	NaN	NaN	1/s2	minimum value of N2					
7	C_shelter	7,60E-01	0,75	1	-	wind sheltering coefficient					
8	swa_b0	2,5	NaN	NaN	1/m	non-PAR light attenuation coefficient for water					
9	swa_b1	1	0,5	1,5	1/m	PAR light attenuation coefficient for water					
10	latitude	59,42	NaN	NaN	dec. deg	lake latitude					
11	longitude	10,83	NaN	NaN	dec. deg	lake longitude					
12	Uz_Sz	0,1	NaN	NaN	m/day	downward settling velocity for passive sedimenting tracer					
13	Uz_Chl	0,064	0,05	0,5	m/day	downward settling velocity for chlorophyll a					
14	Uz_PP	3	1	5	m/day	downward settling velocity for particular phosphorus					
15	alb_melt_ice	0,3	NaN	NaN	-	albedo of melting ice					
16	alb_melt_snow	0,77	NaN	NaN	-	albedo of melting snow					
17	I_scV	1	NaN	NaN	-	scaling parameter for inflow volume					
18	I_scT	1	NaN	NaN	-	scaling parameter for inflow temperature					
19	I_scC	1	NaN	NaN	-	scaling parameter for inflow conc. of C					
20	I_scS	1	NaN	NaN	-	scaling parameter for inflow conc. of S					
21	I_scP	0,5	0,75	1	-	scaling parameter for inflow conc. of P					
22	I_scChl	1	NaN	NaN	-	scaling parameter for inflow conc. of chlorophyll a					
23	I_scPP	0,5	0,75	1	-	scaling parameter for inflow conc. of PP					
24	Y_cp	1	NaN	NaN	-	(chlorophyll to carbon) * (carbon to phosphorus) ratio					
25	m_twty	0,28	0,1	0,3	1/day	specific loss rate at 20 deg C					
26	g_twty	1	0,75	1,5	1/day	specific growth rate at 20 deg C					
27	k_twty	0,28	0,1	0,3	1/day	PP to P transformation rate at 20 deg C					
28	m_sed_twty	0,013	0,0065	0,0195	1/day	chlorophyll a to PP transformation rate in the sediment at 20 deg C					
29	P_half	1	0,5	1,5	mg/m3	half saturation growth P level					
30	PAR_sat	1,16E-04	NaN	NaN	mol(quanta)/ (m2 s)	PAR saturation level for phytoplankton growth					
31	f_par	0,45	NaN	NaN	-	fraction of PAR in incoming solar radiation					
32	beta_chl	0,015	0,0075	0,0225	m2/mg	optical cross-section of chlorophyll					
33	lambda_I	5	NaN	NaN	1/m	PAR light attenuation coefficient for ice					
34	lambda_s	15	NaN	NaN	1/m	PAR light attenuation coefficient for snow					
35	Chl_resusp	0,1	0,1	1	mg/(m2 day)	chlorophyll a resuspension rate					
36	PP_resusp	1,4	0,1	10	mg/(m2 day)	PP resuspension rate					
37											

lake

Ready

Figure 5. *Example of a MyLake parameter file.*

5.3 Switches

The module *solvemodel_v11.m* contains five switches, which can be used to disable some particular model processes. These are:

- snow_compaction_switch (simulation of snow compaction: 0=off, 1=on)
- river_inflow_switch (simulation of river inflow: 0=off, 1=on)

- sedimentation_switch (simulation of sedimentation: 0=off, 1=on)
- sediment_heatflux_switch (simulation of heatflux from sediments: 0=off, 1=on)
- selfshading_switch (simulation of light attenuation by chlorophyll *a*: 0=off, 1=on)
- tracer_switch (simulation of tracer state variables: 0=off, 1=on)

5.4 How to execute a MyLake model run

When the parameter and input data files are ready, a MyLake model application can be run by the following MATLAB command:

[zz,Az,Vz,tt,Qst,dTt,Kzt,Tzt,Czt,Szt,Pzt,Chlzt,PPzt,Qzt_sed,lambdazt,Chlzt_sed,PPzt_sed, Chlzt_sed_sc,PPzt_sed_sc,His,DoF,DoM,MixStat,Wt]= solvemodel_v11(M_start,M_stop,Initfile,Initsheet,Inputfile,Inputsheet,Parafile,Parasheet).

where *M_start* and *M_stop* [year, month, day] are row vectors of the model start and stop date; *Initfile, Inputfile,* and *Parafile* are strings containing the file names (full paths) of the three files containg lake morphometry and initial profiles, time series of meteorological variables and inflow properties, and model parameter values, respectively. Similarly, *Initsheet, Inputsheet,* and *Parasheet* are strings containing the Excel worksheet names containing this data.

For example, using the file examples shown in Figures 3-5 and running the model from May 1, 1998 to December 21, 2000, a model execution line would read:

[zz,Az,Vz,tt,Qst,dTt,Kzt,Tzt,Czt,Szt,Pzt,Chlzt,PPzt,Qzt_sed,lambdazt,Chlzt_sed,PPzt_sed, Chlzt_sed_sc,PPzt_sed_sc,His,DoF,DoM,MixStat,Wt]= solvemodel_v11([1998,5,1],[2000,12,31],'d:\minlake\Vansjo\VAN_init.xls','lake','d:\minlake\Vansjo\ VAN_input71_00.xls','timeseries','d:\minlake\Vansjo\VAN_para_fast_rev.xls','lake');

Note that the whole set of parameter values, initial profiles and input data read from the Excel files (*Parafile, Initfile, Inputfile*) can also be bypassed by entering these variables in correct order directly in the input list after *Parasheet*, i.e:

...=solvemodel_v11(M_start,M_stop,Initfile,Initsheet,Inputfile,Inputsheet,Parafile,Parasheet,In_Z, In_Az, tt, In_Tz, In_Cz, In_Sz, In_Pz, In_Chlz, In_PPz, In_Chlz_sed, In_PPz_sed, Ice0, Wt, Inflow, Phys_par,Phys_par_range, Phys_par_names, Bio_par, Bio_par_range, Bio_par_names)

In other words, the output from model module *modelinputs_v11.m* to *solvemodel_v11.m* is replaced by a similar input directly to *solvemodel_v11.m* given by the user on the command line. The meaning and structure of the output variables from *modelinputs_v11.m* are not explained here, but the user is referred to the header code of that module for detailed information. The possibility to bypass model parameters and other input variables facilitates easier writing of MATLAB scripts for running the model numerous times with different parameter values, e.g. in connection with Monte Carlo simulations and sensitivity analysis.

The model output variables (i.e., from *solvemodel_v11.m*) are listed below with units indicated in square brackets. Output matrix dimensions are indicated in parentheses.

zz	Solution depth domain array (length N) [m], i.e. depths at the top of the layers
Az	Layer interface area [m^2] (N)
Vz	Layer volume [m^3] (N)
tt	Solution time domain array (length M), i.e. model day number, starting from 1 [d]
Qst	Estimated surface heat fluxes [W m^{-2}] ([Q_{sw}, Q_{lw}, Q_{turb}] × M)
dTt	Predicted daily temperature increment [°C] (N × M)
Kzt	Predicted vertical diffusion coefficient [m^2 d^{-1}] (N × M)
Tzt	Predicted temperature profile [°C] (N × M)
Czt	Predicted passive tracer profile [-] (N × M)
Szt	Predicted passive sedimenting tracer profile [-] (N × M)
Pzt	Predicted dissolved inorganic phosphorus (phosphate) profile [μg l^{-1} = mg m^{-3}] (N × M)
Chlzt	Predicted chlorophyll *a* profile [μg l^{-1} = mg m^{-3}] (N × M)
PPzt	Predicted particulate phosphorus profile [μg l^{-1} = mg m^{-3}] (N × M)
Qz_sed	Predicted sediment-water heat flux (normalised values, see page 13) [W m^{-2}] (N × M)
lambdazt	Predicted average total light attenuation coefficient down to depth z [m^{-1}] (N × M)
Chlzt_sed	Predicted content of chlorophyll sediment storage [mg m^{-2}] (N × M)
PPzt_sed	Predicted content of particulate phosphorus sediment storage [mg m^{-2}] (N × M)
Chlzt_sed_sc	Predicted resuspension of chlorophyll [mg m^{-3} d^{-1}] (N × M)
PPzt_sed_sc	Predicted resuspension of particulate phosphorus [mg m^{-3} d^{-1}] (N × M)
His	Ice and snow simulation matrix [m, m, m, °C, °C, kg m^{-3}, boolean] ([h_{ice} h_s h_{si} T_{ice} T_a ρ_s *IceOn/Off*] × M)
DoF	Predicted days of freezing [model day number]
DoM	Predicted days of melting [model day number]
MixStat	Temporary variables used in model testing, see model code (X × M)

Wt Meteorological forcing data (M × variables in columns 4-10 described in section 5.2.1)

Note that the model runtime can easily be reduced by optimising an iteration loop in the turbulent heatflux function (hfbulktc.m) in the *Air-Sea Toolbox* (contact the report authors for more details on this optimisation). Increasing vertical grid step size, and turning off e.g. simulation of the tracers and/or calculation of sediment-water heat fluxes, by using the switches described in section 5.3, will also contribute to shorter runtimes.

6. Examples of model output

Figures 6-8 show some model output (daily values) examples from a case study in which MyLake model code was applied to simulate phosphorus-phytoplankton dynamics in Lake Vansjø (Saloranta et al., 2004). Figure 9 shows a model output from the same case study, but where the simulated daily values from the grid points in the 0-4 m surface layer are averaged to yearly summer means.

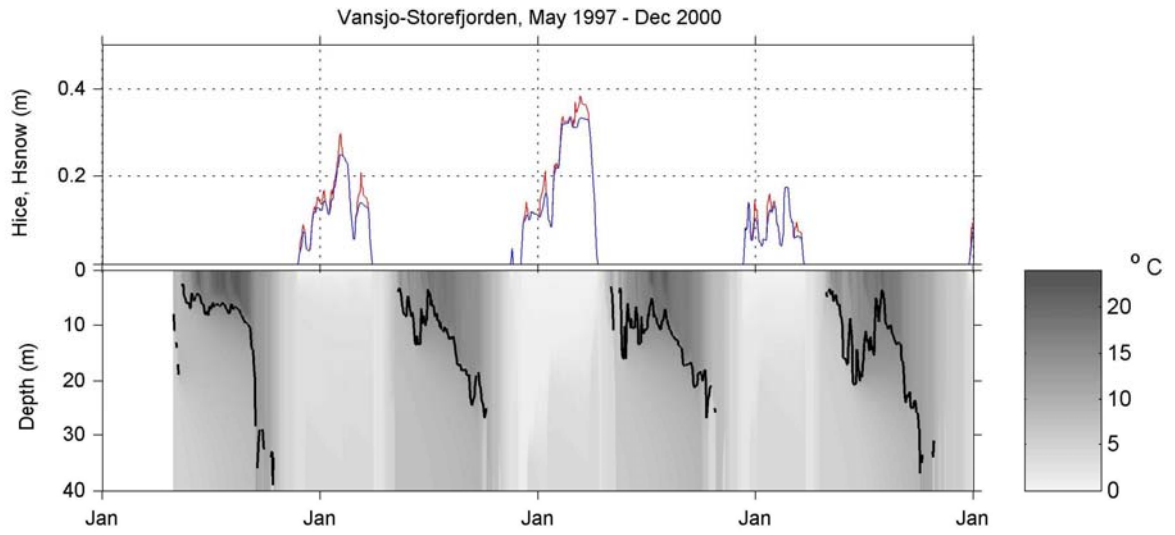

Figure 6. *Upper panel: simulated daily ice (solid lines) and snow thickness (lines drawn on top of ice thickness) in Vansjø-Storefjorden in 1997-2000. Lower panel: simulated daily water temperature profiles. Black lines denote the pycnocline depth.*

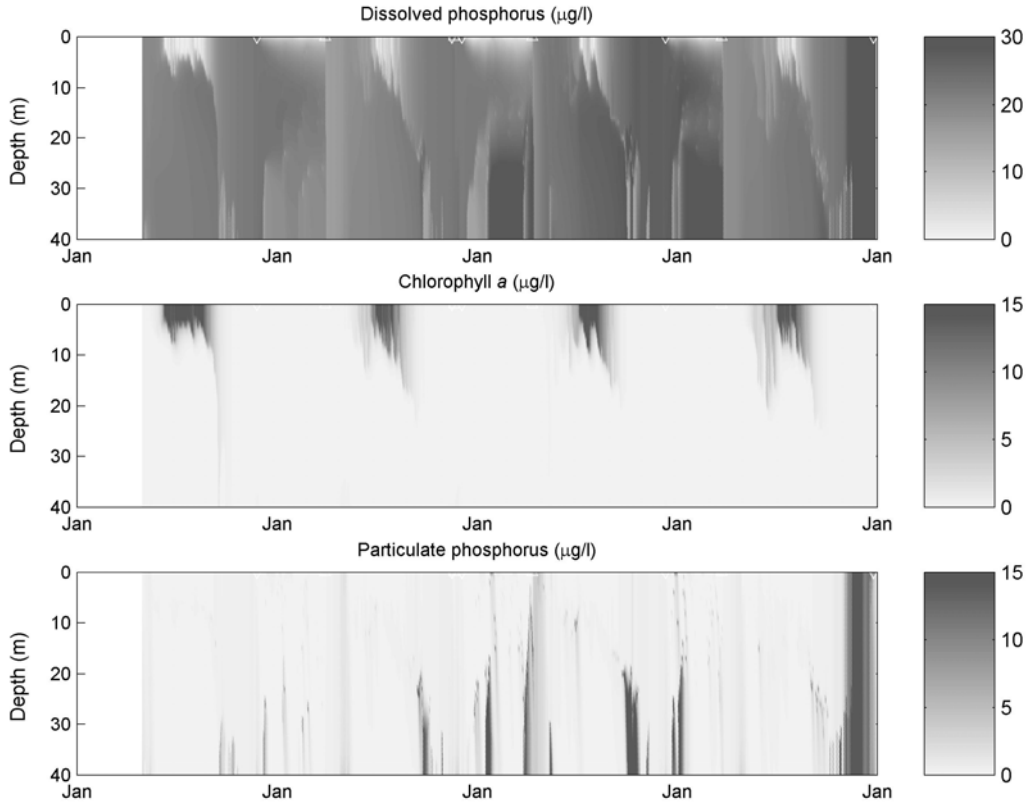

Figure 7. *Simulated daily profiles of (a) phosphate, (b) chlorophyll a, and (c) particulate phosphorus concentrations in Vansjø-Storefjorden in 1997-2000.*

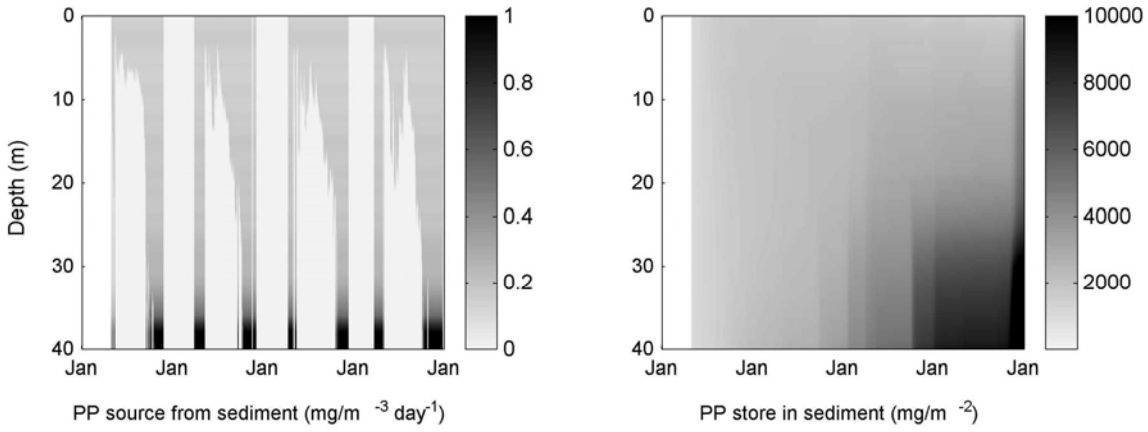

Figure 8. *Simulated daily profiles of (a) resuspension and (b) sediment store content of particulate phosphorus in Vansjø-Storefjorden in 1997-2000.*

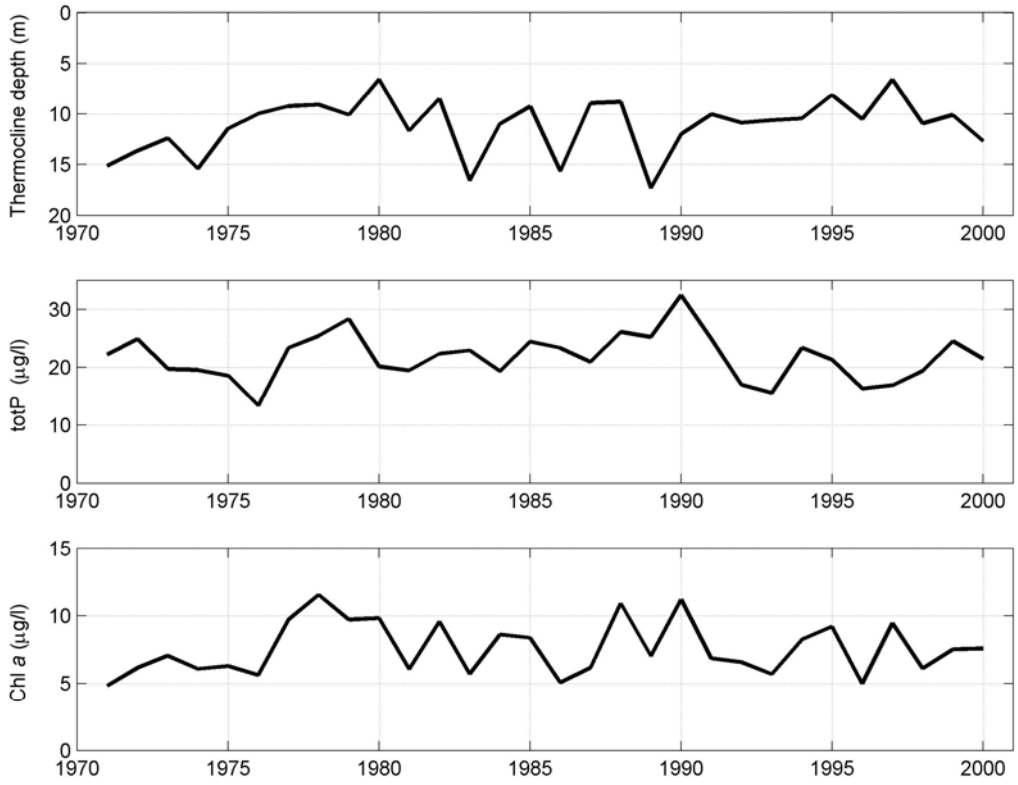

Figure 9. *Simulated (a) mean (Jun-Aug) pycnocline depth, and mean (Jun-Sep, 0-4 m) concentrations of (b) total phosphorus and (c) chlorophyll a in Vansjø-Storefjorden in 1971-2000. Total phosphorus is defined as the sum of phosphate, particulate phosphorus and chlorophyll a expressed in phosphorus units.*

7. References

Dhamotharan, S., J. S. Gulliver, and H. G. Stefan 1981, 'Unsteady one-dimensional settling of suspended sediment', *Water Resources Res. 17*, 1125-1132.

Fang, X., and H. G. Stefan 1996, 'Long-term lake water temperature and ice cover simulations/measurements', *Cold Regions Science and Technology 24, 289-304.*

Ford, D. E., and H. G. Stefan 1980, 'Thermal predictions using integral energy model', *Journal of the Hydraulic Division (ASCE) 106*, 39-55.

Hondzo, M., and H. G. Stefan 1993, 'Lake water temperature simulation model', *Journal of Hydraulic Engineering 119*, 1251-1273.

Kirk, J. T. O. 1983, '*Light and photosynthesis in aquatic ecosystems*', Cambridge University Press, 401 pp.

Leppäranta, M. 1991, 'A review of analytical models of sea-ice growth', *Atmosphere-Ocean 31*, 123-138.

Lydersen et al. 2003, '*THERMOS-prosjektet: Fagrapport 1998-2002*', NIVA rapport 4720-2003, Norwegian Institute for Water Research, Oslo, Norway, 119 pp., in Norwegian.

Perovich, D. 1998, 'The optical properties of sea ice', In M. Leppäranta (ed.), *Physics of ice-covered seas*, Helsinki University Printing House, 195-230.

Reed, R. K. 1977, 'On estimating insolation over the ocean', *J. Phys. Oceanog. 7,* 482-485.

Riley, M. J. and H. G. Stefan 1988, 'MINLAKE: A dynamic lake water quality simulation model', *Ecological Modelling 43*, 155-182.

Saloranta, T. 2000, 'Modeling the evolution of snow, snow ice and ice in the Baltic Sea', *Tellus 52A,* 93-108.

Saloranta, T. M., T. H. Bakken, and A. S. Ibrekk 2004, '*Modelling long-term changes in water quality of Lake Vansjø, Norway: Case story of the application of the models SOBEK and MyLake to Vansjø river basin*', NIVA-rapport, forthcoming in 2004.

UNESCO 1981. International Equation of State of Seawater 1980. UNESCO Technical Papers in Marine Science No 36

Yen, Y-C. 1981, 'Review of thermal properties of snow, ice and sea ice', US Army Cold Regions Research and Engineering Laboratory (CRREL), Report 81-10, Hanover, NH, USA.

Appendix A. Depth- and time-integrated aquatic photosynthesis

The relationship between light and photosynthesis is a fundamental constraint on the growth of autotrophs. The light response of photosynthesis is generally found to be a saturation function, increasing close to linearly in low light and levelling off to an asymptote in high light. Phytoplankton cells experience an exponentially attenuated vertical light gradient, as well as diurnal dark-light cycle increasing from dawn to noon and decreasing until dusk. The average daily photosynthesis in a given depth interval of a lake will thus be the consequence of integrating the light response function over depth and time. There is an obvious need for efficient algorithms for computing the fundamental integrals of phytoplankton growth. This applies in particular vertically structured models solved by fully implicit methods, in which long time steps become feasible and desirable.

We assume that the response of photosynthesis (*P*) to light (*I*) can be described by a monotonously increasing function *F*, with two scaling parameters representing the saturated level of photosynthesis (*P'*) and the saturating light level (*I'*)

$$P = P' \, F\left(I / I'\right)$$

Furthermore, we will assume that light is attenuated exponentially with depth within each layer *i,* with an attenuation coefficient ε_i, and that surface irradiance I_0 is a function symmetrical around solar noon. If light attenuation follows Beer-Lambert's law, then light at a depth $z \in \left[z_i, z_{i+1}\right]$ will be given by

$$I(z,t) = I_{zi}(t)\exp\left(-\varepsilon_i\left(z - z_i\right)\right)$$

with I_{zi} being the irradiance at depth z_i, i.e., at the top of layer *i*.

Day length (λ) can be computed from standard astronomical formulae involving the eccentricity of the earth orbit and the declination of the earth's rotational axis, for any latitude and time of year. We will assume that surface irradiance can be described by a symmetrical function ($G\left(-x\right) = G\left(x\right)$) with two scaling parameters representing surface irradiance at noon (I_0') and day length (λ)

$$I_0(t) = I_0^{'} G\left(2t / \lambda\right)$$

From these premises we can assemble the general depth-time integral of photosynthesis within the layer *i* (i.e., from z_i to z_{i+1})

$$Q_i = \frac{1}{(z_{i+1} - z_i)} \int_{-\frac{\lambda}{2}}^{\frac{\lambda}{2}} \int_{z_i}^{z_{i+1}} P(I(z,t)) dz \; dt$$

$$= \frac{P'}{(z_{i+1} - z_i)} \int_{-\frac{\lambda}{2}}^{\frac{\lambda}{2}} \int_{z_i}^{z_{i+1}} F\left(\frac{I_{zi}}{I'} \exp(-\varepsilon_i (z - z_i)) G(2t/\lambda) \right) dz \; dt$$

By a simple change of variables and by exploiting the symmetry of the diel surface irradiance function and representing the depth integral as a difference between two integrals going to infinity from z_i and z_{i+1}, respectively, this can be written as

$$Q_i = \frac{P' \lambda}{\varepsilon_i (z_{i+1} - z_i)} \left(H\left(\frac{I'_{zi}}{I'} \right) - H\left(\frac{I'_{zi+1}}{I'} \right) \right)$$

with the depth integration contained in the dimensionless function *H*

$$H(u) = \int_0^1 \int_0^\infty F\left(u \, e^{-y} \, G(x) \right) dy \, dx$$

If light saturated production *P'* is given in units of mg C m^{-3} h^{-1}, day length (λ) in h d^{-1} and light attenuation (ε) in m^{-1}, then Q_i will be interpreted as daily production per unit volume (mg C m^{-3} d^{-1}) within layer *i*. For simplicity, we have introduced a general integral *H* representing the integrated production in a hypothetical infinite layer with attenuation coefficient ε. This is just a matter of mathematical convenience; it is the integral over the finite depth interval, represented as the difference between two infinite integrals that has a real significance in the model.

Analytical solution to the double integral defining *H*(*u*) depends on the functional forms of *F* and *G*. Several functions have been proposed for the light response function (*F*), including piece-wise linear, rectangular hyperbola, exponential, and hyperbolic tangent. With a possible exception for the exponential model, which can be derived from an idealised Poisson hit process, all these models are purely empirical. Particularly simple solutions result if we assume a piece-wise linear model, such as

$$F(x)=\begin{cases} x & x\le 1 \\ 1 & x>1 \end{cases}$$

The double integral for H(u) can then be decomposed into 3 integrals over simple sub-regions of the domain ($x\in[0,1]$, $y\in[0,\infty)$) , as illustrated in the figure below

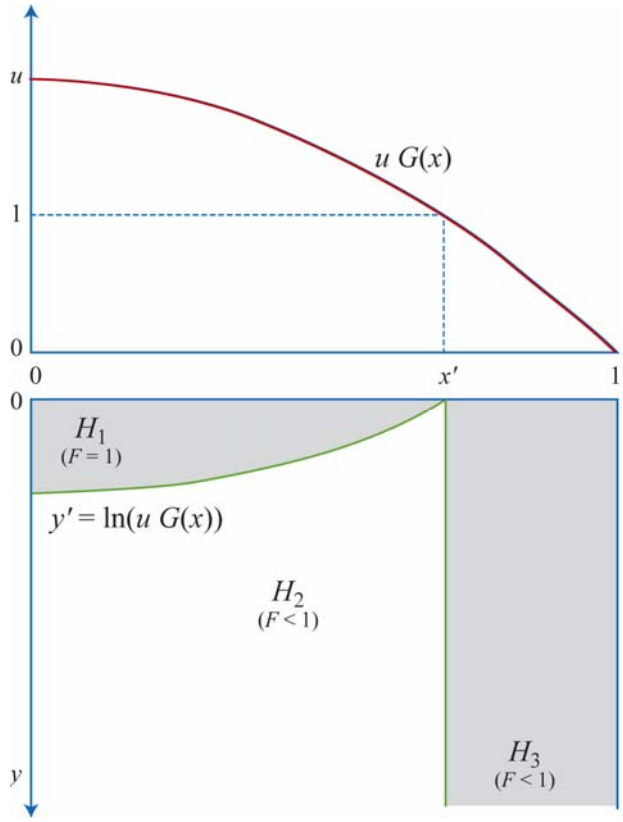

If surface light at noon is sufficient to saturate photosynthesis ($I_0' > I'$), then there will be a (scaled) time interval $0\le x\le x'=G^{-1}\left(u^{-1}\right)$ where photosynthesis is saturated over a (scaled) depth interval $0\le y\le y'=\ln\left(u\,G\left(x\right)\right)$. The integrand in the expression for *H*(*u*) be unity over this region (1). Correspondingly, photosynthesis will be unsaturated in the region 2 defined by $0\le x\le x'$ and $y>y'$, and for all $y\ge 0$ whenever $x'<x\le 1$ (region 3). Regions 1 and 2 will collapse to zero if surface light at noon is sub-saturating ($I_0'\le I'$). The compound integral can be written as $H\left(u\right)=H_1\left(u\right)+H_2\left(u\right)+H_3\left(u\right)$, where *u* is the scaled surface irradiance at noon, and where

$$H_1(u) = \int_0^{x'} \int_0^{y'} dy\, dx$$

$$H_2(u) = u \int_0^{x'} \int_{y'}^{\infty} G(x) \exp(-y)\, dy\, dx$$

$$H_3(u) = u \int_{x'}^{1} \int_0^{\infty} G(x) \exp(-y)\, dy\, dx$$

So far we have said little about the function $G(x)$, except that it should be symmetrical. We can restrict it further by requiring it to be monotonously decreasing and possibly convex. An inverted parabola is one of the simplest functions that fit these criteria, and which will make the analytical solution for $H(u)$ particularly simple:

$$G(x) = 1 - x^2$$

Boundaries between sub-regions are given by $x' = \sqrt{1-u^{-1}}$ and $y' = \ln\left(u\left(1-x^2\right)\right)$ for this choice of function. The corresponding integrals can be solved as follows

$$\begin{aligned} H_1(u) &= \int_0^{x'} \ln\left(u\left(1-x^2\right)\right) dx \\ &= \int_0^{x'} \left[\ln(u) + \ln(1+x) + \ln(1-x)\right] dx \\ &= \ln\left(1+\sqrt{1-u^{-1}}\right) - \ln\left(1-\sqrt{1-u^{-1}}\right) - 2\sqrt{1-u^{-1}} \end{aligned}$$

$$\begin{aligned} H_2(u) &= u \int_0^{x'} \left(1-x^2\right) \int_{y'}^{\infty} \exp(-y)\, dy\, dx \\ &= u \int_0^{x'} \left(1-x^2\right) \exp\left(-y'(x)\right) dx = \int_0^{x'} dx = \sqrt{1-u^{-1}} \end{aligned}$$

$$\begin{aligned} H_3(u) &= u \int_{x'}^{1} \left(1-x^2\right) \int_0^{\infty} \exp(-y)\, dy\, dx \\ &= u \int_{x'}^{1} \left(1-x^2\right) dx = \tfrac{2}{3} u - \tfrac{1}{3}(2u+1)\sqrt{1-u^{-1}} \end{aligned}$$

Assembling the sub-domain components, and noticing that regions 1 and 2 collapse whenever $u < 1$ gives the final expression for the double integral:

$$H(u) = \begin{cases} \frac{2}{3}u & u \le 1 \\ \frac{2}{3}u + \ln\frac{\sqrt{u}+\sqrt{u-1}}{\sqrt{u}-\sqrt{u-1}} - \frac{2}{3}(u+2)\frac{\sqrt{u-1}}{\sqrt{u}} & u > 1 \end{cases}$$

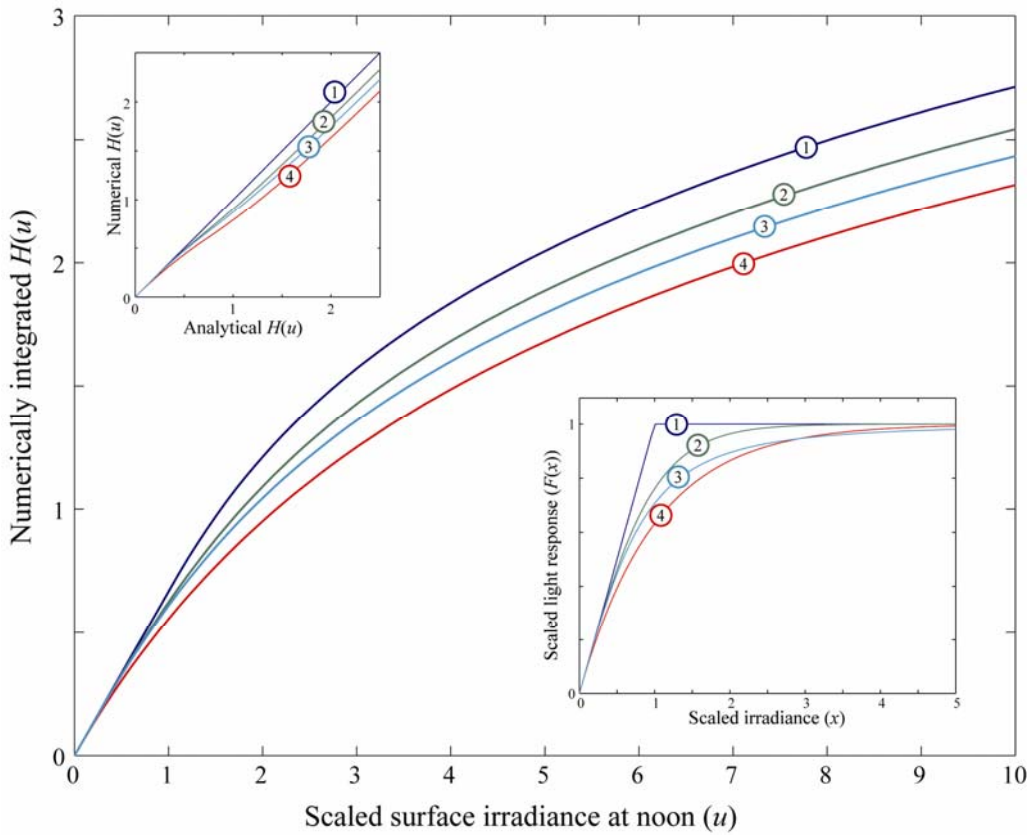

The figure above shows that the scaled photosynthesis integral is smooth even when the light response function is piecewise linear. Moreover, it has basically the same shape for several proposed light response functions (lower insert) including the widely applied Poisson hit model (4; ref), as well as functions introduced by Vollenweider 1974 (3) and by Jassby & Platt 1976 (2). The upper insert shows that there is a close to linear relationship between the analytically derived solution and the numerically integrated models. Thus, the Poisson hit model (4) can be approximated by 0.83 $H(u)$ with a RMS error of 0.037. Likewise, the models of Vollenweider and Jassby & Platt can be approximated by 0.88 $H(u)$ and 0.92 $H(u)$, with RMS errors of 0.021 and 0.019, respectively.

References

Jassby, A. D., Platt, T. 1976. Mathematical formulation of relationship between photosynthesis and light for phytoplankton. Limnol. Oceanogr. 21 (4): 540-547

Vollenweider, R. A. 1974. A manual on methods for measuring primary production in aquatic environments. IBP Handbook No 12 (2^{nd} edition) 225 pp.